



Interpreting the past, providing for the future

EXPLANATION

CORRELATION OF MAP UNITS

Qal	Qac	Qs	Holocene	QUATERNARY	CENOZOIC
Twdr	Qg	Pleistocene	PALEOGENE		
Unconformity				Eocene	MESOZOIC
Unconformity			Paleocene		
Unconformity				CRETACEOUS	
Unconformity					
Unconformity				JURASSIC	
Unconformity					
Unconformity				PALEOZOIC	
Unconformity					
Unconformity				PRECAMBRIAN	
Unconformity					

DESCRIPTION OF MAP UNITS

Cenozoic

- Qal** Alluvium (Holocene)—Unconsolidated to poorly consolidated, subangular to subrounded, locally derived sand, silt, clay, and gravel. Includes modern floodplain and associated terrace deposits along Poison Spider Creek, Cleveans Draw, Iron Creek, and tributaries. Thickness generally less than 14 m.
- Qac** Alluvium and colluvium (Holocene and Pleistocene)—Unconsolidated to poorly consolidated, locally derived sand, gravel, silt, and clay. Includes slopewash and alluvial fan deposits along western flank of Oil Mountain. Thickness undetermined.
- Qs** Windblown sand (Holocene and Pleistocene)—Tan to white, very fine to coarse-grained, poorly sorted, subrounded to rounded, unconsolidated quartz sand with minor components of very fine, angular to subangular heavy minerals. Often overlain by thin silty soil. Forms east-west-trending band of vegetated landforms north of Poison Spider Creek. Thickness generally less than 14 m.
- Qg** Terrace gravels (Pleistocene?)—Unconsolidated pebbles, cobbles, and boulders in silty sand matrix. Abundant white, gray, and brown quartzite, with minor components of maroon and greenish quartzite; white, gray, and brown chert sandstone; and granite. Forms flat benches about 20–30 m above modern grade of Poison Spider Creek. Very thin, unannexed gravel lag present on nearby bedrock surfaces of similar elevation. Exposed thickness generally less than 5 m.
- Twdr** Wind River Formation (Eocene)—Informally divided into three distinct facies. Upper facies poorly indurated pebble- to boulder-conglomerate composed of subangular to rounded clasts of variably colored quartzite, granite, and chert with minor components of petrified wood, in a silty to coarse-grained arkosic matrix. Granite boulders up to 50 cm in diameter. Thickness of upper facies unknown. Middle facies, drab-brown to gray siltstones and 0.3- to 0.6-m-thick, rusty-brown, well-indurated lenticular sandstones; carbonaceous siltstone and variegated red, white, and gray mudstone near base; about 90 m thick. Lower facies, light gray-brown to pale-yellow, arkosic, occasionally cross-bedded, commonly poorly bedded conglomeratic sandstone interbedded with red and white mudstone; wood fragments common; about 30 m thick. Upper facies caps plateau to southeast; exposures of lower and middle facies limited to base of escarpment in southwestern map area. Angular unconformity with underlying Fort Union Formation. Full thickness not observed in quadrangle; thickens west of Casper arch thrust. Nearby well logs suggest total thickness greater than 800 m.
- Tu** Fort Union Formation (Paleocene)—Interbedded mudstone and sandstone with conglomerate, carbonaceous shale, and siltstone. Mudstone and siltstone, light-gray to gray-brown, occasionally gray-green, interbedded with thin bentonitic mudstones. Iron concretions common, increasing upward. Sandstone, white to buff and friable, or brown, ferruginous, and well-indurated, fine- to coarse-grained, moderately to well-sorted, subangular, cross-bedding common; occasional leaf fossils; lenticular, generally 0.5–2 m thick. Conglomerate lenses, rusty-brown, contain occasional chert and porcellanite pebble clasts; increasingly arkosic upward. Carbonaceous shale, waxy-brown, with abundant wood fragments and occasional thin lenticular coals. Forms drab gray badlands punctuated by sandstone hogback ridges. Basal contact with underlying Lance Formation indistinct, marked by slight angular unconformity. Lowermost 810 m observed.

Mesozoic

- Kl** Lance Formation (Upper Cretaceous)—Interbedded mudstone and sandstone with siltstone, carbonaceous shale, and coal. Sandstone, white-tan to dark-gray weathering brown to maroon, very fine to coarse-grained, moderately to poorly sorted, angular to subangular, occasionally calcareous, and of variable induration. Typically plane-bedded, with occasional flaser and trough cross-bedding. Bed laterally continuous in lower part becoming lenticular upward, generally 0.5–2 m thick. Abundant ripple marks and rare mud cracks, occasional iron concretions throughout. Mudstones white-yellow and brown-purple. Siltstones light-brown to orange. Carbonaceous shale, dark-brown with occasional wood fragments. Rare lenses of trough cross-bedded pebble conglomerate near upper contact. Approximately 880–900 m thick.
- Km** Metcete Formation (Upper Cretaceous)—Interbedded mudstone, carbonaceous shale, coal, siltstone, and sandstone. Carbonaceous shale, drab-brown and friable. Mudstone, brown to purple-gray, contains abundant root traces and wood fragments. Sandstone, commonly brown-gray weathering tan-orange, fine- to medium-grained, poorly to moderately sorted, subangular to subgranular, calcareous, moderately well indurated, about 0.5–2 m thick. Bedding includes thin planar beds, tabular or trough cross-beds, and moderately thick massive beds. Basal sandstone, distinct gray-white, weathering pale-blue-gray, very friable, about 8 m thick. Intercalated with upper and lower tongues of Lewis Shale. Poorly exposed. Approximately 150–155 m thick.
- Klc** Lewis Shale (Upper Cretaceous)—Drab-gray shale interbedded with thin sandstones, siltstones, tan-gray, weathering orange-gray, very fine to medium-grained, poorly sorted, angular to subrounded, moderately well indurated, plane-bedded with occasional cross-beds. Common shell hash lenses, trace fossils, and rare *Baculites* fossils. Upper and lower shale tongues bound intercalated Metcete Formation. Both tongues poorly exposed, typically concealed beneath thick soil. Basal contact with underlying Trapper Sandstone conformable, locally marked at top of lenticular, orange-brown, ferruginous, well-indurated sandstone. Upper tongue approximately 85–90 m thick. Lower tongue approximately 120 m thick.
- Kmnu** Mesaverde Formation (Upper Cretaceous)
- Kmnp** Teapot Sandstone—White-gray, medium- to fine-grained, fining upward, subangular to subrounded, moderately well sorted, moderately friable sandstone. Abundant quartz, lithic fragments, and heavy minerals give distinct "salt and pepper" appearance. Tough cross-bedding and ripple-scale cross-bedding throughout. Occasional soft-sediment deformation, burrow traces, and iron concretions less than 2 cm in diameter. Coal, about 0.5-m-thick, near base. Unconformable basal contact with underlying unnamed middle member. Forms prominent northeast-southwest-trending hogback ridge elevated 5–8 m above surrounding topography. Approximately 30 m thick.
- Kmnu** Unnamed middle member—Interbedded mudstone, carbonaceous shale, siltstone, and sandstone. Mudstone and shale, white-gray to gray, poorly exposed. Siltstone, tan-brown, gray, poorly exposed. Sandstone, gray to brown, weathering rusty-brown, very fine to fine-grained, moderately to well sorted, subangular to rounded. Plane-bedded with abundant breakage, occasional rounded weathering. Beds more laterally continuous near base, becoming lenticular upward. Common wood fragments and iron concretions. Approximately 165 m thick.
- Kmnp** Parkman Sandstone—Sandstone, interbedded with silty sandstone and carbonaceous shale. Sandstone, gray to yellow, weathering tan, very fine to fine-grained, poorly to moderately sorted, calcareous, subangular to subrounded. Abundant quartz with occasional heavy minerals and lithic fragments. Plane-bedding common in lower parts, with blocky to fluggy breakage; trough cross-beds more common up section. Occasional ripple marks, abundant trace fossils and shell hash lenses, common spherical weathering up to 2 m diameter associated with well-indurated ferruginous sandstones. Carbonaceous shale and mudstone beds increase up section; occasional plant fossils. Locally exposed as rounded mounds of cross-bedded sandstone, poorly exposed in most of map area. Approximately 35 m thick.
- Kmnc** Fales Sandstone and Wallace Creek Tongue of Cody Shale, undivided—Fales Sandstone is poorly exposed sandstone at base of Mesaverde Formation, separated from overlying Parkman Sandstone by drab-gray Wallace Creek Tongue of Cody Shale, which also contains similar, indistinct, poorly exposed sandstones. Identity of Fales Sandstone inferred from nearby well logs. Sandstones, generally pale-tan-gray weathering light- to dark-brown, medium- to coarse-grained, friable, poorly to moderately well sorted, subangular to subrounded, somewhat calcareous, 0.5- to 2-m-thick. Bedding typically planar or planar non-parallel, with some cross-bedding. Occasional trace fossils and shell fragments. Approximately 250 m thick.
- Kc** Cody Shale (Upper Cretaceous)—Shale with thin sandstones, siltstones, and chalky marls. Shale is drab gray to light brown, weathers gray, with thin irregular beds of ironstone throughout. In upper half, three to four thin sandstones and silty sandstones, orange to brown weathering, tan to gray, fine- to medium-grained, moderately to poorly sorted, angular to subangular, with abundant quartz and feldspar, lithic fragments, and heavy minerals. Sandstones typically plane-bedded but flaser, wavy discontinuous, and tabular cross-bedding also present. Occasional trace fossils and ripple marks. In lower half, three to six pale-gray to bluish-white chalky marl horizons with occasional shell fragments, corresponding to "Niobrara equivalent" of Finn (2017). Forms broad, relatively flat expanses with poor exposure. Basal contact sharp, possibly unconformable. Approximately 1,100 m thick.
- Kab** Sage Breaks Shale (Upper Cretaceous)—Dark-gray, poorly exposed shale containing distinct, abundant, lenticular to spherical septarian nodules 0.3–1.2 m in diameter. Occasional thin horizons of gray, weathering orange, siltstone. Approximately 100 m thick.

Frontier Formation (Upper Cretaceous)

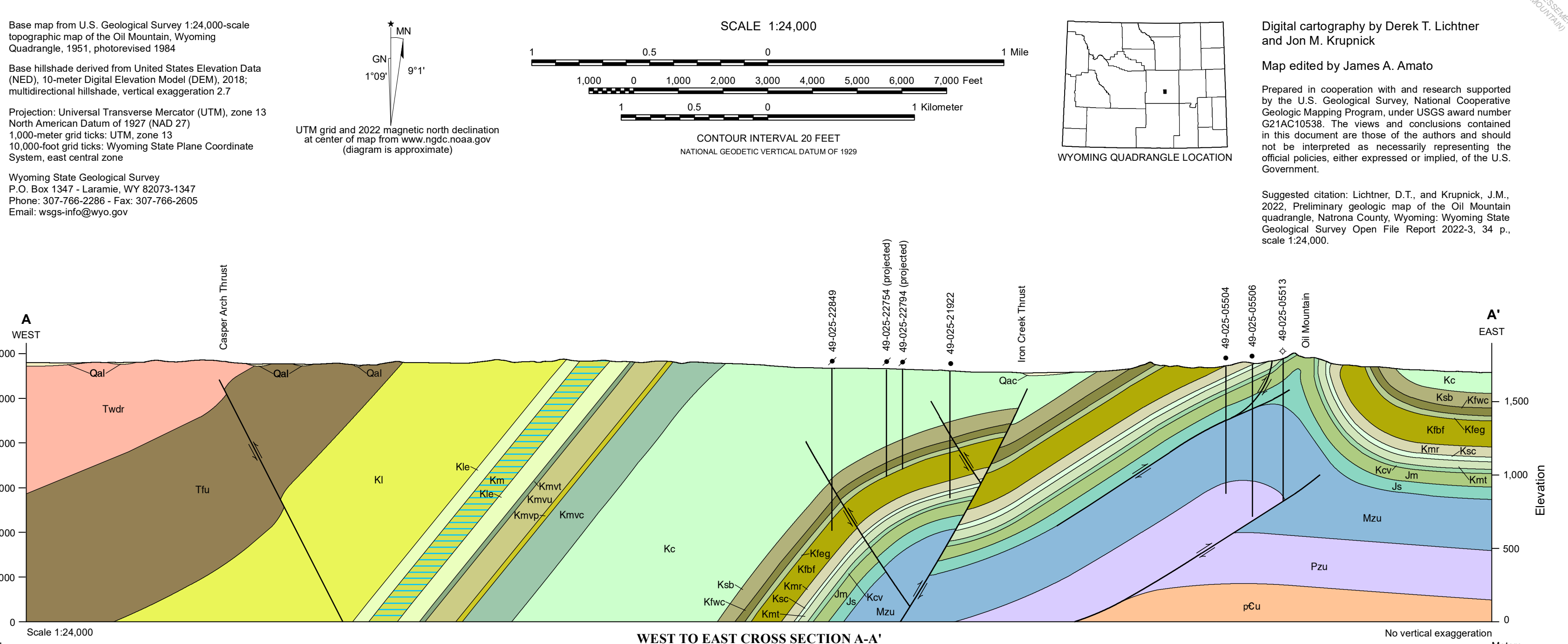
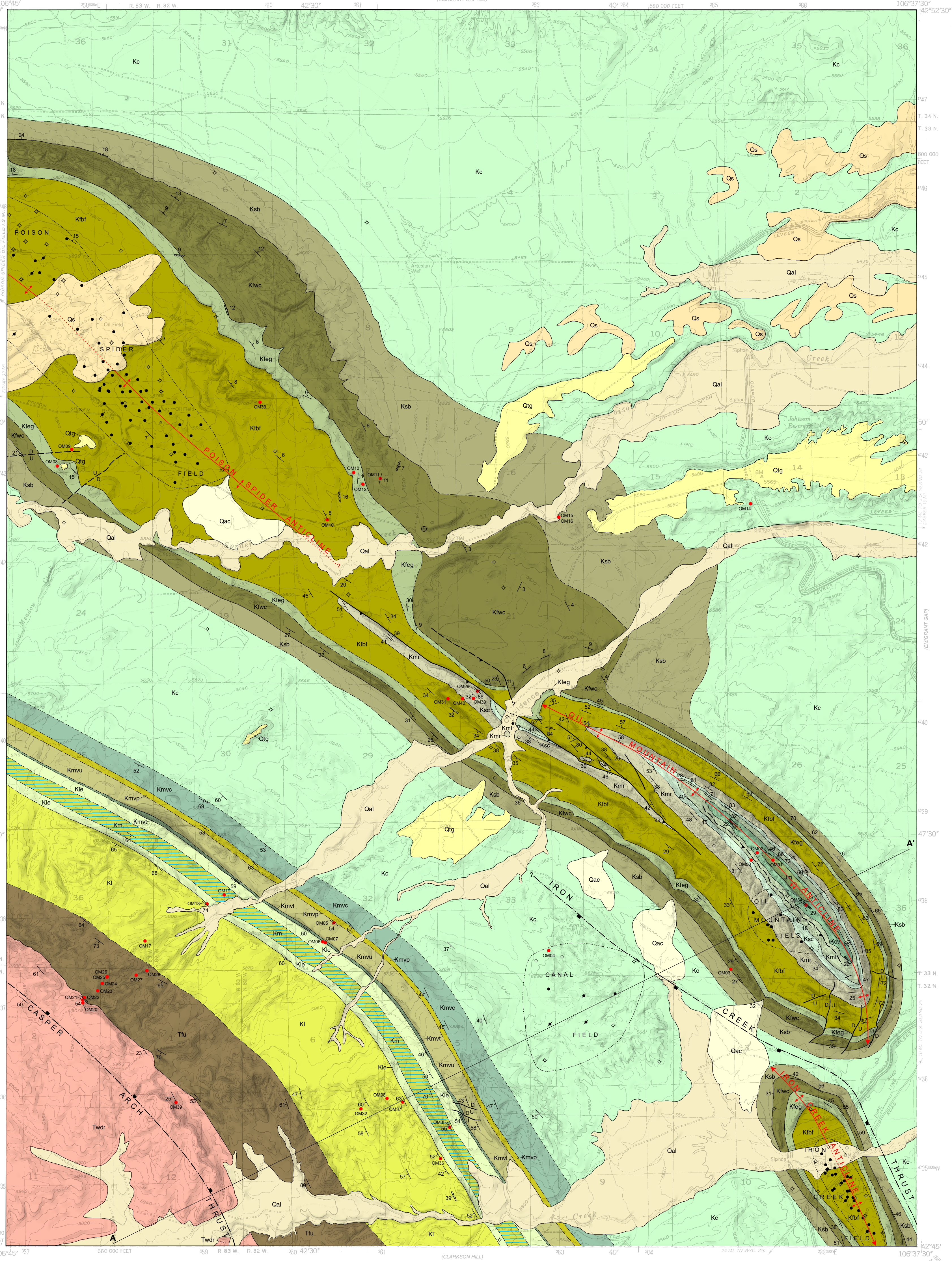
- Kwan** Wall Creek Member—Coarsening upward sequence of shale and sandstone. Sandstone, white-gray to buff-tan, weathering tan, fine- to medium-grained, coarsening-upward, subangular to subrounded, well-sorted, plane-bedded near base, cross-bedded in upper portions. Moderately friable, increasingly friable up section. Trace fossils and shell fossils common, including *Panora*. Occasional well-indurated lenses of orange-brown cross-bedded sandstone. Forms prominent northeast-trending hogback ridge of Oil Mountain anticline; where flat lying weathers into distinct butts and hoodoos. Basal contact unconformable, very indistinct, about poorly exposed thin sandstone at top of underlying Emigrant Gap Member. Approximately 55 m thick.
- Kleg** Emigrant Gap Member—Interbedded black to gray, friable, poorly exposed shale and thin, poorly exposed sandstone intercalated with distinct 1.5-m-thick white-gray to tan, weathering brown, very fine to medium-grained, poorly to moderately sorted, subangular to subrounded, moderately to well-indurated, calcareous conglomeratic sandstone with abundant quartz, occasional heavy minerals and lithic fragments. Irregular planar beds and cross-bedding throughout. Abundant well rounded dark-gray and black chert pebbles. Fossilized shark teeth common. Occasional spherical weathering up to 2 m in diameter associated with well-indurated sandstone. Basal contact unconformable, about locally distinct 1- to 2-m-thick light-gray bentonitic mudstone of underlying Belle Fourche Member. Approximately 35–45 m thick.
- Kblf** Belle Fourche Member—Three to four coarsening-upward sequences of shale, bentonitic mudstone, and siltstone capped by prominent sandstones. Sandstones, white-tan, weathering rusty-brown, occasionally ferruginous, very fine to medium-grained, subangular to subrounded, moderately well to poorly sorted, friable to well-indurated, dominated by quartz with abundant heavy minerals. Common thin plane-bedding with occasional tabular, trough, and ripple cross-beds. Intervals between sandstones poorly exposed, consisting of interbedded gray to black carbonaceous shale, friable gray and tan silty sandstone, and light-brown mudstone. Siltstone and silty sandstone, commonly nonbedded, with occasional pelecypod molds. In lowermost prominent sandstone, spherical weathering up to 3 m diameter. Lower 60 m of shale contains abundant ellipsoid ironstone concretions up to 1 m in diameter, and numerous bentonitic mudstones. Sharp, conformable basal contact with underlying Mowry Shale. Total thickness approximately 180 m.
- Kmnr** Mowry Shale (Upper Cretaceous)—Gray to black, fissile, siliceous shale and siltstone, occasionally weathering to mottled white, orange, or brown. Abundant fish scales, rare ammonite fragments, vertebrate fossils, and cone-in-cone structures. Siliceous shale capped by locally distinct, very well indurated, very fine grained silty calcareous sandstone overlain by Clay Spur Bentonite, a regionally pervasive, 2-m-thick waxy yellow bed with common popcorn weathering. Forms distinct slopes of well-indurated siliceous silver-colored plates. Basal contact gradational. Approximately 70–80 m thick.
- Ksc** Shell Creek Shale (Upper Cretaceous)—Dark-gray to black friable shale interbedded with thin yellow bentonitic beds. Poorly exposed. Previously mapped elsewhere in region as lower part of Mowry Shale or upper part of Thermopsis Shale. Approximately 30–35 m thick.
- Kmt** Muddy Sandstone and Thermopsis Shale, undivided (Lower Cretaceous)—Muddy Sandstone is moderately well indurated, pebble-tan, fine- to medium-grained, poorly to moderately well sorted, massive calcareous quartz arenite, approximately 12 m thick, with occasional heavy minerals and common carbonaceous shale stringers. Plane-bedded, occasionally cross-bedded, with occasional asymmetric ripple marks. Forms a subangular sandstone ridge flanked by shale valleys. Sharp, erosional contact with underlying Thermopsis Shale. A drab gray-brown to dark-gray, poorly exposed shale interbedded with thin, silty sandstones containing abundant trace fossils. Lowermost 2.5 m poorly exposed rusty-red mudstone. Total undivided thickness approximately 60 m.
- Kcv** Cloverly Formation (Lower Cretaceous)—Tan to peach, coarse-grained, angular to subangular sandstone, with abundant trough cross-bedding, underlain by tan-buff, fining-upward basal conglomerate containing subrounded to rounded blue-gray chert, brown-gray quartz, white quartz, and minor amounts of other sedimentary lithic fragments. Sandstone and conglomerate friable to moderately indurated with mottled red staining throughout. Forms prominent cliffs flanking axis of Oil Mountain anticline. Basal contact unconformable. Approximately 25–35 m thick.
- Jm** Morrison Formation (Jurassic)—Dully variegated red-purple, yellow-brown, white-gray, and blue-green friable mudstone containing lenticular, white-gray, moderately well sorted, very fine to fine-grained, quartz-rich, cross-bedded sandstone and silty sandstone. Exposed along axis of Oil Mountain anticline. Approximately 85 m thick in well logs.
- Ja** Sundance Formation (Jurassic)—Only in cross section
- Mzu** Older Mesozoic units, undivided—Only in cross section

Paleozoic

- Pzu** Paleozoic units, undivided—Only in cross section

Precambrian

- pCu** Precambrian units, undivided—Only in cross section



PRELIMINARY GEOLOGIC MAP OF THE OIL MOUNTAIN QUADRANGLE, NATRONA COUNTY, WYOMING

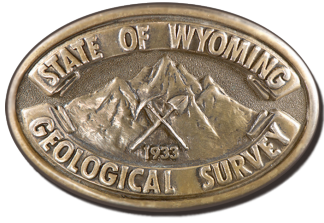
by
Derek T. Lichtner and Jon M. Krupnick
2022

NOTICE TO USERS FOR OPEN FILE REPORTS
Open File Reports are preliminary and usually require additional fieldwork and/or compilation and analysis; they are meant to be a first release of information for public comment and review. The Wyoming State Geological Survey welcomes any comments, suggestions, and contributions from users of the information.

DISCLAIMERS
Users of this map are cautioned against using the data at scales different from those at which the map was compiled. Using these data at a larger scale will not provide greater accuracy and is a misuse of the data. The Wyoming State Geological Survey (WSGS) and State of Wyoming make no representation or warranty, expressed or implied, regarding the use, accuracy, or completeness of the data presented herein, or of a map printed from these data. The act of distribution shall not constitute such a warranty. The WSGS does not guarantee the digital data or any map printed from the data to be free of errors or inaccuracies. The WSGS and State of Wyoming disclaim any responsibility or liability for interpretations made from, or any decisions based on, the digital data or printed map. The WSGS and State of Wyoming retain and do not waive sovereign immunity. The use of or reference to trademarks, trade names, or other product or company names in this publication is for descriptive or informational purposes only, or is pursuant to licensing agreements between the WSGS or State of Wyoming and software or hardware developers/vendors, and does not imply endorsement of those products by the WSGS or State of Wyoming.

REFERENCES
Cerna, E.G., Kerns, G.J., and Laraway, W.J., 1983. Bedrock geologic map of the Pine Mountain-Oil Mountain area, Natrona County, Wyoming. U.S. Geological Survey Open-File Report 83-748, 18 p., 4 pls., scale 1:31,680.
Finn, T.M., 2007. Subsurface stratigraphic cross sections of Cretaceous and lower Tertiary rocks in the Wind River Basin, central Wyoming. chap. 9 of U.S. Geological Survey Wind River Basin Province Assessment Team, comp., Petroleum systems and geologic assessment of oil and gas in the Wind River Basin province, Wyoming. U.S. Geological Survey Digital Data Series DDS-69-J, 28 p., 11 pls.
Finn, T.M., 2017. Stratigraphic cross sections of the Niobrara interval of the Cody Shale and associated rocks in the Wind River Basin, central Wyoming. U.S. Geological Survey Scientific Investigations Map 3370, 19 p., 1 pl.
General Petroleum Corp., 1954. Geologic map of South Casper Creek, Poison Spider, Oil Mountain, Iron Creek, Natrona County, Wyoming, scale 1:36,026, in Olson, W.G., ed.: Wyoming Geological Association, Ninth annual field conference, Guidebook, 83 p., 10 pls.
Hers, C.J., Ball, M.W., Clair, S.S., Reeside, J.B., Heald, K.C., and Collins, A.C., 1946. Geologic map of the southeastern part of the Wind River Basin and adjacent areas in central Wyoming. U.S. Geological Survey Preliminary Map 51, scale 1:126,720.
Henning, P.H., Olson, J.E., and Thompson, L.B., 2000. Combining outcrop data and three-dimensional structural models to characterize fractured reservoirs—An example from Wyoming. American Association of Petroleum Geologists Bulletin, v. 84, no. 6, p. 830-849.
Hunter, John, Ver Ploeg, A.J., and Boyd, C.S., 2005. Geologic map of the Casper 30' x 60' quadrangle, Natrona and Converse counties, central Wyoming. Wyoming State Geological Survey Map Series 65, scale 1:100,000.
Johnson, R.C., 2007. Detailed measured sections, cross sections, and paleogeographic reconstructions of the Upper Cretaceous and lower Tertiary non-marine interval, Wind River Basin, Wyoming. chap. 10 of U.S. Geological Survey Wind River Basin Province Assessment Team, comp., Petroleum systems and geologic assessment of oil and gas in the Wind River Basin province, Wyoming. U.S. Geological Survey Digital Data Series DDS-69-J, 43 p., 6 pls.
Johnson, R.C., Finn, T.M., Keefe, W.R., and Szmagaj, R.J., 1996. Geology of Upper Cretaceous and Paleocene gas-bearing rocks, Wind River Basin, Wyoming. U.S. Geological Survey Open-File Report 96-090, 120 p., 3 pls.
Keefe, W.R., 1965. Stratigraphy and geologic history of the uppermost Cretaceous, Paleocene, and lower Eocene rocks in the Wind River Basin, Wyoming. U.S. Geological Survey Professional Paper 495-A, p. 77, 4 pls., scale 1:289,700.
Keefe, W.R., 1970. Structural geology of the Wind River Basin, Wyoming. U.S. Geological Survey Professional Paper 495-D, 35 p., 3 pls., scale 1:250,000.
Keefe, W.R., 1972. Frontier, Cody, and Mesaverde formations in the Wind River and southern Big Horn basins, Wyoming. U.S. Geological Survey Professional Paper 495-E, 22 p., 3 pls.
Love, J.D., 1948. Mesozoic stratigraphy of the Wind River Basin, central Wyoming. Wyoming Geological Association, Third annual field conference, Guidebook, p. 96-111.
Nightingale, E.J., 1990. Structural and stress analysis of the Oil Mountain anticline, Natrona County, Wyoming. Akron, Ohio: University of Akron, M.S. thesis, 69 p.
Rich, E.I., 1962. Reconnaissance geology of Hilland-Clarkson Hill area, Natrona County, Wyoming. U.S. Geological Survey Bulletin 1107-G, p. 447-537, 4 pls., scale 1:31,680.
Soister, E.P., 1968. Stratigraphy of the Wind River Formation in south-central Wind River Basin, Wyoming. U.S. Geological Survey Professional Paper 594-A, 50 p., 5 pls., scale 1:63,560.
Stone, D.S., 2002. Morphology of the Casper Mountain uplift and related subsidiary structures, central Wyoming—Implications for Laramide kinematics, dynamics, and crustal inheritance. American Association of Petroleum Geologists Bulletin, v. 86, no. 8, p. 1,417-1,440.
Wyoming Oil and Gas Conservation Commission, 2021. Wyoming Oil and Gas Conservation Commission, accessed October 2021, at <http://wocgc.state.wy.us/>.

Base map from U.S. Geological Survey 1:24,000-scale topographic map of the Oil Mountain, Wyoming Quadrangle, 1951, photorevised 1984.
Base hillshade derived from United States Elevation Data (NED), 10-meter Digital Elevation Model (DEM), 2018; multidirectional hillshade, vertical exaggeration 2.7.
Projection: Universal Transverse Mercator (UTM), zone 13 North American Datum of 1983 (NAD 83).
1,000-meter grid ticks: UTM, zone 13, 10,000-foot grid ticks: Wyoming State Plane Coordinate System, east central zone.
UTM grid and 2022 magnetic north declination at center of map from www.ngdc.noaa.gov (diagram is approximate).
Wyoming State Geological Survey
P.O. Box 1347, Laramie, WY 82073-1347
Phone: 307-786-2286 • Fax: 307-786-2005
Email: wsgs-info@wyo.gov

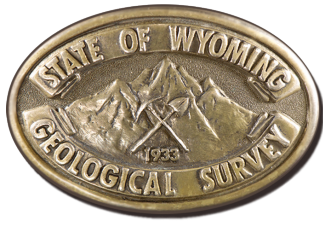


Interpreting the past, providing for the future

Preliminary Geologic Map of the Oil Mountain Quadrangle, Natrona County, Wyoming

Derek T. Lichtner and Jon M. Krupnick

Open File Report 2022-3
June 2022



Wyoming State Geological Survey

Erin A. Campbell, Director and State Geologist



Preliminary Geologic Map of the Oil Mountain Quadrangle, Natrona County, Wyoming

Derek T. Lichtner and Jon M. Krupnick

Layout by Christina D. George

Open File Report 2022-3
Wyoming State Geological Survey
Laramie, Wyoming: 2022

Open File Reports are preliminary and usually require additional fieldwork and/or compilation and analysis; they are meant to be a first release of information for public comment and review. The Wyoming State Geological Survey welcomes any comments, suggestions, and contributions from users of the information.

Citation: Lichtner, D.T., and Krupnick, J.M., 2022, Preliminary geologic map of the Oil Mountain quadrangle, Natrona County, Wyoming: Wyoming State Geological Survey Open File Report 2022-3, 34 p., scale 1:24,000.

Table of Contents

Introduction	1
Location	1
Geologic Setting.	1
Previous Work	1
Methods.	3
Geologic Overview	4
Regional Tectonics	4
Geologic Structure in the Oil Mountain Quadrangle	4
Depositional History Overview	6
Depositional Environments	6
Morrison Formation	6
Cloverly Formation	6
Thermopolis Shale and Muddy Sandstone.	7
Shell Creek Shale and Mowry Shale.	7
Frontier Formation	8
Sage Breaks Shale and Cody Shale	11
Mesaverde Formation	12
Lewis Shale and Meeteetse Formation	15
Lance Formation	16
Fort Union Formation.	18
Wind River Formation	20
Oligocene and Miocene formations	21
Pleistocene terraces and aeolian deposits	21
Holocene alluvium and colluvium	22
Economics	22
Water Resources.	22
Surface Water	22
Groundwater.	22
Oil and Gas	24
Heavy-Mineral Sands.	25
Coal	25
Uranium	25
Industrial Minerals.	26

Analytical Results	26
Geochemistry.	26
Source-Rock Analysis.	26
Palynomorph Biostratigraphy	27
Detrital Zircon Geochronology	27
Acknowledgments	29
References	30

List of Figures

Figure 1. Map of regional geology.	2
Figure 2. Hinge of Oil Mountain anticline	5
Figure 3. Variegated terrestrial sediments of the Morrison Formation	6
Figure 4. Cross-bedded Cloverly Formation sandstone	7
Figure 5. Basal pebble conglomerate of the Cloverly Formation.	7
Figure 6. Muddy Sandstone, looking southwest.	7
Figure 7. Contact between the Mowry Shale and Belle Fourche Member of the Frontier Formation	8
Figure 8. Mowry Shale and the Frontier Formation.	9
Figure 9. Belle Fourche Member sandstone	10
Figure 10. Chert-pebble conglomeratic sandstone in the Emigrant Gap Member of the Frontier Formation	10
Figure 11. Wall Creek Member	10
Figure 12. Streamcut of Sage Breaks Shale.	11
Figure 13. Poorly exposed Cody Shale	12
Figure 14. Upper Cody Shale sandstone	12
Figure 15. Parkman Sandstone	13
Figure 16. Carbonaceous shales in the unnamed middle member of the Mesaverde Formation	13
Figure 17. Unnamed middle member of the Mesaverde Formation	14
Figure 18. Teapot Sandstone of the Mesaverde Formation	14
Figure 19. Teapot Sandstone Member, Lewis Shale, Meeteetse Formation, and Lance Formation.	15
Figure 20. Meeteetse Formation	16
Figure 21. Interbedded sandstone, siltstone, coal, and carbonaceous shale in the lower Lance Formation	17
Figure 22. Poorly exposed upper Lance Formation	17
Figure 23. Lower Fort Union Formation, looking southeast along strike	18
Figure 24. Middle Fort Union Formation.	19
Figure 25. Upper Fort Union Formation ferruginous pebble conglomerate outcrop	19
Figure 26. Wind River Formation	20

Figure 27. Pleistocene terrace21
Figure 28. Kernel density estimate plots of detrital zircon age distributions29

List of Tables

Table 1. Source-rock analysis results27
Table 2. Depositional ages determined from palynomorph biostratigraphy.27
Table 3. Detrital zircon sample locations and youngest-single-grain ages28

INTRODUCTION

Location

The Oil Mountain 7.5-minute quadrangle is west of Casper in Natrona County, central Wyoming. The map area can be reached from downtown Casper by taking U.S. Highway 26 north about 6 miles and turning left onto Zero Road (Co. Rd. 202), which becomes Poison Spider Road (Co. Rd. 201) after 6.5 miles. Poison Spider Road crosses the central and northern parts of the quadrangle, while Oregon Trail Road (Co. Rd. 319) provides access to the southern map area. The quadrangle is a mixture of private, federal, and state lands; landowner permission is required to access outcrops located on or across private land. A network of oil field roads and private two-track roads crisscrosses the area. Many outcrops are accessible only by foot.

Geologic Setting

The Oil Mountain quadrangle is at the intersection of Laramide structures, bridging the western margin of the Casper Arch and the southeastern margin of the Wind River Basin (Keefer, 1970). The Casper Arch, a north-west-trending region of Laramide faulting and folding, separates the Wind River Basin in the west from the Powder River Basin in the east (fig. 1). The Oil Mountain anticline, after which the quadrangle is named, was generated by multiple east-vergent, antithetic thrusts related to the west-vergent Casper Arch thrust.

The bedrock stratigraphy exposed in the Oil Mountain quadrangle ranges from Upper Jurassic through early Eocene. The oldest geologic unit is the Jurassic Morrison Formation; its soft mudstones underlie the topographic basin at the core of the Oil Mountain anticline. The youngest unit, the shallowly dipping Eocene Wind River Formation, is found near the southwestern limit of the map, where it unconformably overlies the Paleocene Fort Union Formation.

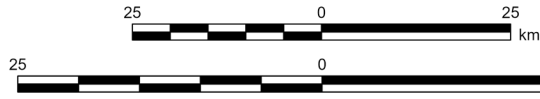
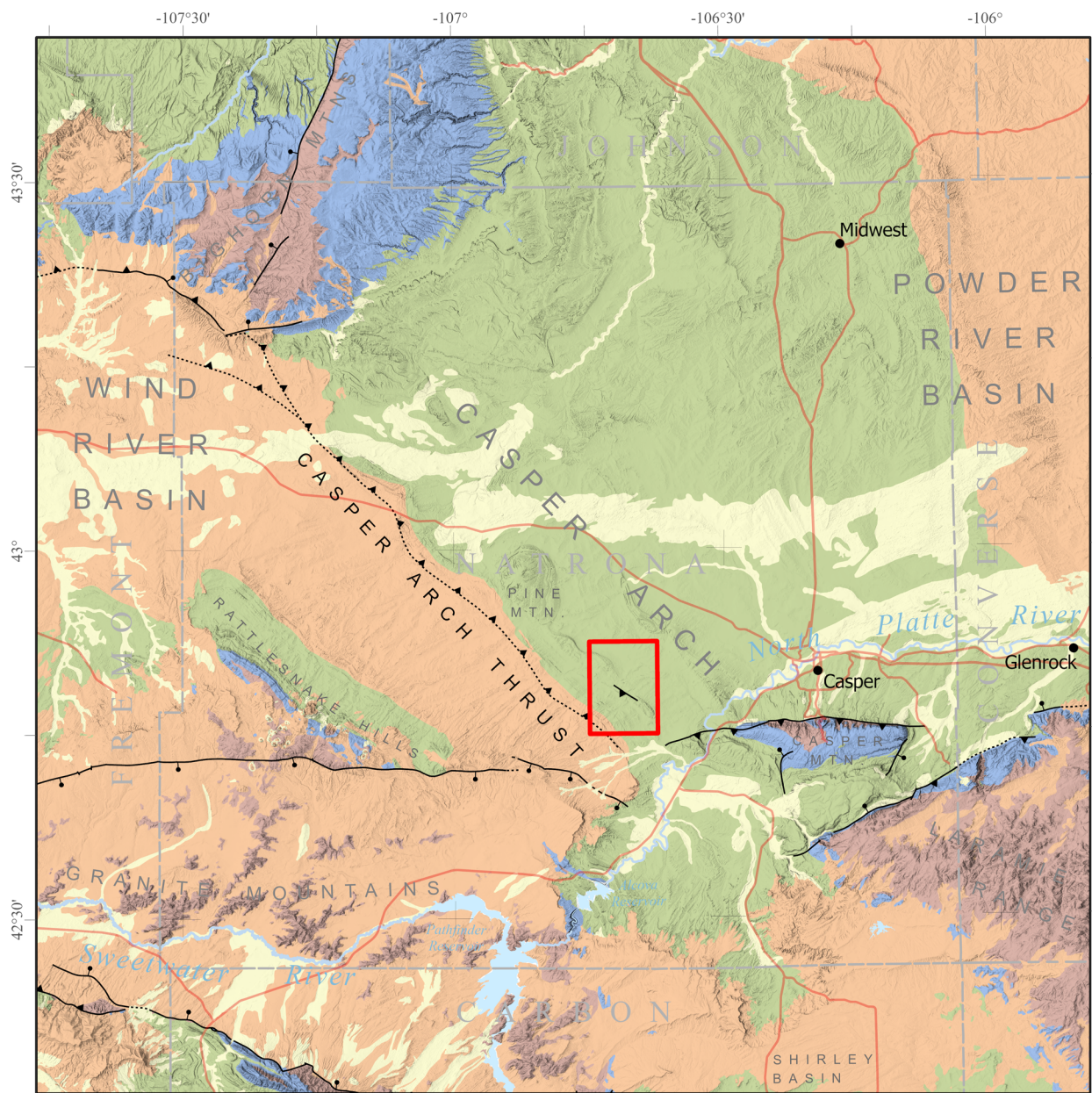
The primary motivation for mapping the Oil Mountain quadrangle is study of sedimentation trends before, during, and after the transgression of the Western Interior Seaway across the Rocky Mountain region in the Late Cretaceous, and of the Sevier and Laramide tectonics that influenced these trends. In addition to shedding light on the geologic history of Wyoming, knowledge of the quadrangle's sedimentary and tectonic history may aid investigation of any mineral resources that occur in the Oil Mountain quadrangle or in similar rocks or geologic structures elsewhere in the region. Several of the geologic units are known oil and gas reservoirs or source rocks in the nearby Wind River and Powder River basins. These same units also may be local sources of groundwater or enriched in mineral resources such as uranium, titanium, or rare earth elements.

Previous Work

The first geologic map to feature Oil Mountain anticline was a 1:126,720-scale bedrock map of the southeastern Wind River Basin, originally published in 1916 and later republished by Hares and others (1946). The map covers large portions of Natrona, Fremont, and Carbon counties.

A guidebook for the ninth annual field conference of the Wyoming Geological Association, edited by Olson (General Petroleum Corporation, 1954), includes a photocopy of a map of the South Casper Creek, Poison Spider, and Iron Creek oil fields at an estimated scale of 1:36,000. This map, by an unknown author, was sourced from the exploration library of General Petroleum Corporation in Los Angeles, California, and depicts the Oil Mountain anticline, including structure contours at the top of the Dakota Sandstone (Cloverly Formation), structural measurements, major faults, and major unit contacts (General Petroleum Corporation, 1954).

A publication by Rich (1962) examines the geology of the Hiland-Clarkson Hill area in Natrona County. Included in this publication is a 1:31,680-scale map that borders the southern portion of the Oil Mountain quadrangle and a 1:250,000-scale map that includes the Upper Cretaceous and Paleogene strata in the southwestern part of the Oil Mountain quadrangle.



EXPLANATION

MAP SYMBOLS		GEOLOGIC UNITS
County boundary	Oil Mountain quadrangle	Quaternary
Major road	Fault—continuous where certain, dotted where concealed; sawteeth on upper plate of thrust fault; ball and bar on downthrown block of normal fault	Paleogene and Neogene
City or town		Mesozoic
Water		Paleozoic
		Precambrian

Figure 1. Map of regional geology, showing major faults, landforms, outcrop, and the extent of the Oil Mountain quadrangle.

Keefer (1965) published a bedrock map of the Wind River Basin at a scale of about 1:250,000, with a focus on uppermost Cretaceous through lower Eocene stratigraphy. Units mapped near Oil Mountain include the Fort Union Formation and an undivided unit consisting of the Lance and Meeteetse formations and Lewis Shale. A later map by Keefer (1970) depicts the structural geology of the Wind River Basin at a scale of 1:250,000.

Cserna and others (1983) of the U.S. Geological Survey published an open-file report and associated map, at a scale of approximately 1:31,680, showing several key bedrock contacts in the Pine Mountain-Oil Mountain area.

Hunter and others (2005) from the Wyoming State Geological Survey published a 1:100,000-scale bedrock map of the Casper quadrangle in Natrona and Converse counties. The map includes the Oil Mountain quadrangle and compiled information from the above sources.

Hennings and others (2000) examined the fracture history of the Oil Mountain anticline. This study included seismic profiles and several cross sections depicting the surface and subsurface geology. Structural measurements acquired by Nightengale (1990) for a master's thesis were used by Hennings and others (2000) in their analysis.

Methods

Mapping was carried out from July through September 2021. Aerial imagery, digital elevation models, topographic maps, subsurface well data, regional stratigraphic correlations, and previously published geological maps of various scales were used to supplement field observations.

Rock samples were collected for various laboratory analyses: uranium-lead (U-Pb) detrital-zircon geochronology, palynomorph biostratigraphy, whole rock geochemistry, total organic carbon and pyrolysis, and examination of thin sections under a microscope.

Detrital-zircon samples were collected from the Lance, Fort Union, and Wind River formations to provide insight on sediment provenance and to better constrain depositional age. Sampling targeted immature sandstones. Three samples underwent U-Pb detrital-zircon analysis at the Arizona LaserChron Center.

Samples for palynomorph biostratigraphy were collected from the terrestrial Meeteetse, Lance, Fort Union, and Wind River formations. Distinctive pollen assemblages were used to infer the age and depositional environment of these formations (Nichols, 2003). Sample collection was based on several criteria: deposition in quiescent environments, exposure to reducing rather than oxidizing environments, and minimal alteration. A majority of the samples were from carbonaceous shales, from fresh exposure where possible to avoid contamination by contemporary pollen. Twelve samples were submitted for processing, analysis, and interpretation to Biostratigraphy.com, LLC.

Whole rock geochemistry samples were collected throughout the quadrangle. A majority of the samples were sandstones, but shales and conglomerates were also sampled. Fifteen samples were submitted to ALS Geochemistry for geochemical analysis.

Samples for analysis of total organic carbon and pyrolysis were collected from the Mowry Shale, Belle Fourche Member of the Frontier Formation, and Cody Shale. These analyses can provide insight on the potential of these units as hydrocarbon source rocks in the nearby Wind River and Powder River basins, as well the thermal and burial history of strata along the Casper Arch. Seven samples were submitted to ACT Labs for source-rock analysis.

Samples from the Cloverly Formation, Muddy Sandstone, Frontier Formation, Cody Shale, Mesaverde Formation, Lewis Shale, and Meeteetse, Lance, Formation Union, and Wind River formations were sent to Wagner Petrographic for thin section creation, with the aim of better characterizing mineralogy, understanding provenance, and examining diagenesis. In addition to 15 standard thin sections with blue-epoxy impregnation, five polished thin sections were made for use in reflected-light microscopy and scanning-electron microscopy.

A ZIP archive containing supplemental data tables can be downloaded from the WSGS publications webpage.

GEOLOGIC OVERVIEW

Regional Tectonics

Beginning in the Late Jurassic, subduction of the Farallon plate beneath North America produced the Sevier orogenic belt along the western margin of the continent (Picard, 1993; DeCelles, 2004). Shortening, thickening, and loading of the crust resulted in flexural subsidence in the Sevier foreland, allowing the Western Interior Seaway to inundate the continental interior during much of the Cretaceous (Steidtmann, 1993; DeCelles, 2004).

Near the end of the Late Cretaceous, the subduction angle of the Farallon plate shallowed, resulting in Laramide-style thick-skinned deformation, characterized by northwest–southeast-oriented, basement-involved reverse faults (English and Johnston, 2004; Liu and others, 2010). In this time of overlapping Sevier and Laramide deformation styles, dynamic subsidence, caused by mantle downwelling associated with flat-slab subduction of the Farallon plate, played a large role in determining patterns of subsidence and uplift in the Sevier foreland (Li and Aschoff, 2022; Minor and others, 2022). Pulses of Laramide uplift continued from roughly 80 Ma (mega annum or million years) to around 40 Ma, partitioning the Sevier foreland into the pattern of Laramide uplifts and basins observed today. Early movement of some Laramide uplifts, such as the Wind River Range and Granite Mountains, likely began in the Maastrichtian (Flemmings and Nelson, 1991; Fan and Carrapa, 2014). By the Paleocene, rapid uplift along the Casper Arch and other Laramide structures was well underway (Flemmings and Nelson, 1991; Carroll and others, 2006; Fan and Carrapa, 2014). By the early Eocene, Paleozoic and Mesozoic strata had eroded from the highest Laramide uplifts, exposing the Precambrian basement (Carroll and others, 2006; Fan and others, 2011).

Post-Laramide regional uplift, during which the mountains and basins of the Rocky Mountain region together were lifted to near-present elevations, commenced sometime in the late Miocene. Explanations for this widespread yet poorly understood tectonic event involve a combination of broad-scale, domal uplift related to mantle buoyancy and isostatic rebound due to extensive erosion of upper Eocene, Oligocene, and lower Miocene deposits (McMillan and others, 2006). With the removal of Laramide compressive stresses around this time, localized extension and arch collapse also occurred, resulting in the collapse of the Granite Mountains in central Wyoming and backsliding along some basin-bounding thrusts (Thompson, 2015).

Geologic Structure in the Oil Mountain Quadrangle

The Oil Mountain quadrangle is at the western margin of the Casper Arch, along the Oil Mountain-Pine Mountain lineament (Cserna and others, 1983; Stone, 2002). The northeast-dipping Casper Arch thrust, in the southwestern corner of the quadrangle, is a regional, basin-bounding reverse fault separating the Wind River Basin from the Casper Arch.

The Iron Creek thrust, in the southeastern corner of the quadrangle, is a southwest-dipping reverse fault in the hanging wall of the Casper Arch thrust. It cores the basement-involved, asymmetric, northwest-trending Iron Creek anticline (Hennings and others, 2000). To the northwest, the Iron Creek thrust terminates near the surface in the Cody Shale. Multiple fault splays dip in the northeast direction, controlling oil and gas production at the Canal and Iron Creek oil fields. The Poison Spider anticline, in the northwestern portion of the map area, is likewise a northwest-trending asymmetrical fold in the hanging wall of the Casper Arch thrust.

The asymmetric, basement-detached, doubly plunging, tightly folded Oil Mountain anticline is the most prominent geologic structure in the quadrangle (fig. 2). The Oil Mountain anticline is cored by two low-angle thrust faults that dip to the southwest: a deep detachment in Cambrian strata and a shallow detachment in the evaporite-rich beds of the Chugwater Formation (Hennings and others, 2000). A splay from this upper detachment reaches the surface along the backlimb of the anticline. In the southern portion of the Oil Mountain anticline, several splays and a few small tear faults are exposed at the surface.

Several small structures are present elsewhere in the quadrangle. A pair of west–northwest-trending faults in the south-central region of the map offsets the Lewis Shale and upper members of the Mesaverde Formation. A pair of east-trending and northeast-trending faults offsets the Frontier Formation in the northwestern corner of the map area, along the backlimb of the Poison Spider anticline. In the central portion of the quadrangle, a number of unmapped meter-scale folds are present in the Mowry and Shell Creek shales and Frontier Formation, adjacent to northwest-trending detachment faults along the Oil Mountain-Pine Mountain lineament.

Hennings and others (2000) studied in detail fracture trends in the Oil Mountain anticline. Northwest-striking fractures, found throughout the region in the Wall Creek Member of the Frontier Formation, are hypothesized to have formed prior to the Laramide orogeny, for the spacing of these fractures is not affected by the degree of deformation in the Oil Mountain anticline (Hennings and others, 2000). One proposed mechanism for the creation of this set of fractures is mild extension during the eastward migration of the Sevier forebulge. Thompson (2015), however, suggests that this fracture orientation actually does not predate the Laramide orogeny, and is instead a result of Laramide and post-Laramide tectonic activity.

The second set of major fractures in the Oil Mountain anticline strikes in the northeast direction. These fractures formed as a product of folding and deformation of the anticline, a hypothesis supported by variation in the saturation of fractures with the local degree of deformation (Hennings and others, 2000).

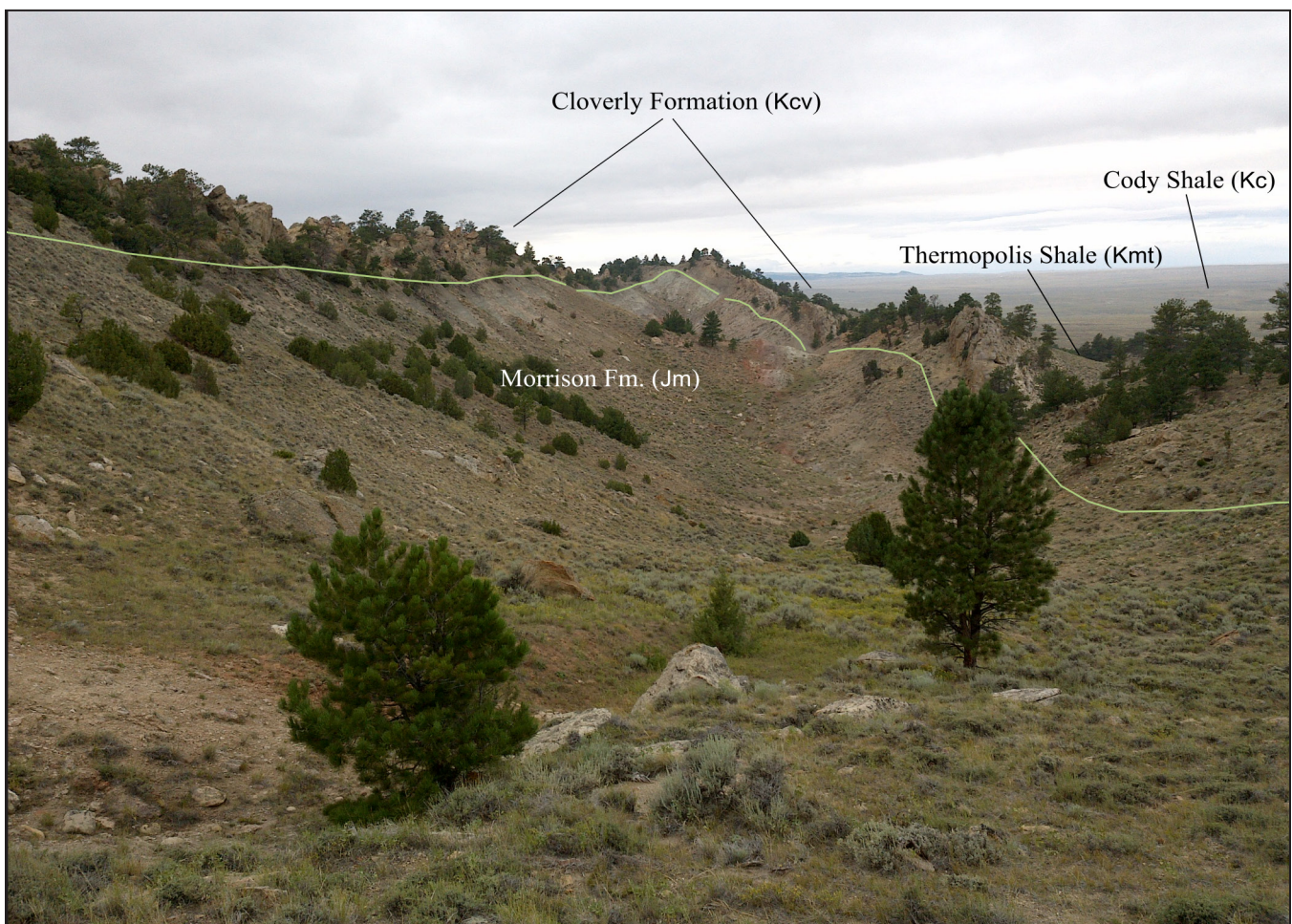


Figure 2. Annotated photograph along hinge of Oil Mountain anticline, looking northwest, SW¼NE¼ sec. 35, T. 33 N., R. 82 W.

Depositional History Overview

Jurassic- through Eocene-age sedimentary rocks are exposed in the Oil Mountain quadrangle. The terrestrial deposition of the Jurassic and lowermost Cretaceous units occurred in the Sevier foreland (DeCelles, 2004). Marine and marginal-marine strata of the Upper Cretaceous were deposited during the transgressive-regressive cycles of the Western Interior Seaway in response to global eustatic sea level changes and local tectonics (Shapurji, 1978; Steidtmann, 1993; Li and Aschoff, 2022; Minor and others, 2022). Paleocene and lower Eocene strata were deposited in intracontinental basins adjacent to actively deforming Laramide uplifts (Keefer, 1965; Fan and others, 2011). No upper Eocene through Miocene sediments or volcanics, which occur elsewhere in the region (Rich, 1962), are preserved in the Oil Mountain quadrangle. The Quaternary record consists of Pleistocene terrace deposits, aeolian dune deposits, and recent alluvium and colluvium. Some of these Quaternary deposits have since been dissected, while others are still being formed today.

Depositional Environments

In addition to interpretations of depositional environment for each geologic unit, this section provides additional observations not included in the map plate's Description of Map Units.

Morrison Formation

The Jurassic Morrison Formation is exposed only along the axis of the Oil Mountain anticline, where its relatively soft mudstones eroded to form a topographic depression flanked by the more erosion-resistant Cloverly Formation (fig. 3). Deposition of the Morrison Formation occurred in a terrestrial environment with a seasonal climate characterized by sporadic rainfall and dry seasons (Picard, 1993). Sediments were sourced from Sevier uplifts to the west and southwest. The colorful lithology of this unit consists of fining-upward sequences that record soil formation and deposition in ephemeral lakes, braided and meandering fluvial channels, floodplains, and alluvial fans (Picard, 1993). Rare vertebrate bone fragments were observed in outcrop at Oil Mountain. In the very center of the anticline there is a 6,000-m² patch of soil with distinctive weathering characteristics and vegetation that may be a small, unmapped exposure of Jurassic Sundance Formation; no trenching was conducted to verify the parent material of this soil.

Cloverly Formation

The soft mudstones of the Morrison Formation are unconformably overlain by the sandstones (fig. 4) and conglomerates (fig. 5) of the Neocomian- to Albian-age Cloverly Formation. This Lower Cretaceous unit forms the dual ridges flanking the axis of Oil Mountain anticline. The Cloverly Formation preserves remnants of fluvial drainages that carried sands and gravels northeast from the Sevier orogenic belt into the Sevier foreland basin (Steidtmann, 1993).



Figure 3. Photograph of variegated terrestrial sediments of the Morrison Formation. Looking southeast along strike, NE¼NW¼ sec. 35, T. 33 N., R. 82 W.



Figure 4. Photograph of cross-bedded Cloverly Formation sandstone, southwest flank of Oil Mountain, NW $\frac{1}{4}$ NW $\frac{1}{4}$ sec. 35, T. 33 N., R. 82 W. Sample OM-DL20210727-2A was collected at this location.



Figure 5. Photograph of basal pebble conglomerate of the Cloverly Formation, SW $\frac{1}{4}$ NE $\frac{1}{4}$ sec. 35, T. 33 N., R. 82 W. Sample OM-DL20210820-1A was collected at this location.

Thermopolis Shale and Muddy Sandstone

The Thermopolis Shale first appears in the sedimentary record as a bed of red-weathering mudstone that represents a transitional environment between the terrestrial deposition of the Cloverly Formation and the marine deposition of the Thermopolis Shale. The dark-colored fine-grained sediments of the Thermopolis Shale were deposited during the Kiowa-Skull Creek transgression-regression cycle, which marks the first inundation of the North American continent by the Cretaceous Western Interior Seaway (Steidtmann, 1993). When the seaway regressed, there was extensive subaerial exposure and significant erosion and incision of the Thermopolis Shale (Curry, 1985).

Paleovalleys of dissected Thermopolis Shale were subsequently filled by the sediments of the Muddy Sandstone (fig. 6). The Muddy Sandstone was deposited first as fluvial sediments, and then as marginal-marine and marine sediments when the continental interior was again flooded during the Greenhorn transgression-regression cycle (Curry, 1985; Steidtmann, 1993). The Grieve Paleovalley, a north–northwest–trending paleovalley extending from near Casper Mountain into the interior of the Wind River Basin, consists of fluvial sands in the lowest sections, marine muds and sands high in the paleovalley, and muds containing plant material in areas of high paleorelief (Curry, 1985). The outcrop at Oil Mountain consists of plane-bedded to massive sandstones with fragments of organic plant material and occasional asymmetrical current ripples. Nearby outcrops of the Muddy Sandstone represent beach, shoreline, and marginal marine environments (Curry, 1985).



Figure 6. Photograph of Muddy Sandstone, looking southwest, NW $\frac{1}{4}$ SE $\frac{1}{4}$ sec. 35, T. 33 N., R. 82 W.

Shell Creek Shale and Mowry Shale

The continued transgression of the Greenhorn cycle led to the deposition of the Shell Creek Shale and Mowry Shale during the early Cenomanian. The Shell Creek Shale is dark colored and non-siliceous, while the overlying Mowry Shale is cemented with silica and bright silver to dark gray in color (fig. 7). During deposition of the Shell Creek Shale, the Mowry Sea remained open to the north but was bounded to the south by the transcontinental arch, which

separated it from the proto-Gulf of Mexico and prevented significant ocean currents (Steidtmann, 1993). The dark color and high organic content of the Shell Creek and Mowry shales are products of these deep, stagnant waters (Steidtmann, 1993). The bentonite beds throughout this interval and the siliceous and porcellanitic characteristics of the Mowry Shale relate to continued volcanic activity during this time (Steidtmann, 1993).

The Shell Creek Shale has been mapped elsewhere in the region as either the lower part of the Mowry Shale (Hintze, 1915; Love, 1948) or upper part of the Thermopolis Shale (Lupton, 1916; Harshman, 1972; Curry, 1985). Because of the erosional contact of the Muddy Sandstone with the underlying Thermopolis Shale (the “lower part” of some authors), the Shell Creek interval is more appropriately grouped with the overlying Mowry Shale, with which it has a gradational contact, or as a separate unit where mappable, as in the Oil Mountain quadrangle.



Figure 7. Annotated photograph of the contact between the Mowry Shale and Belle Fourche Member of the Frontier Formation, looking north, NE $\frac{1}{4}$ NW $\frac{1}{4}$ sec. 28, T. 33 N., R. 82 W. This area also contains numerous small faults and folds that are not mappable at a scale of 1:24,000.

Frontier Formation

As sea level rose, the Mowry Sea overtopped the transcontinental arch, forming the Greenhorn Sea, which rose to its maximum level in the early Turonian. The Frontier Formation (fig. 8) was deposited along the margin of the Greenhorn Sea in a variety of marine, marginal-marine, and shallow-marine depositional environments (Merewether and others, 1979; Merewether, 1983; Steidtmann, 1993). Across Wyoming, the depositional environments, thicknesses, and location of unconformities are variable within the Frontier Formation, as transgression and regression of the Greenhorn Seaway were affected by local tectonism (Merewether, 1983; Steidtmann, 1993). In the Oil Mountain quadrangle, the coarsening-upward, southward-prograding shallow-marine sequences of shale and sandstone in the

Belle Fourche Member (fig. 9), supplied by contemporaneous uplift and erosion in the Sevier orogenic belt to the west, were deposited as sea level rose (Merewether and Cobban, 1986). The chert-pebble conglomeratic sandstones and shales of the Emigrant Gap Member (fig. 10) were deposited in deltaic nearshore environments during local transgression and then regression on an erosional surface following slight uplift in the early to middle Turonian throughout much of Wyoming (Merewether and Cobban, 1986). Slight uplift and erosion in eastern Wyoming occurred again in the middle to late Turonian, after which the coarsening-upward shales and marine-shelf sandstones of the Wall Creek Member (fig. 11) were deposited during continued sea-level rise in the late Turonian to middle Coniacian (Merewether and Cobban, 1986).

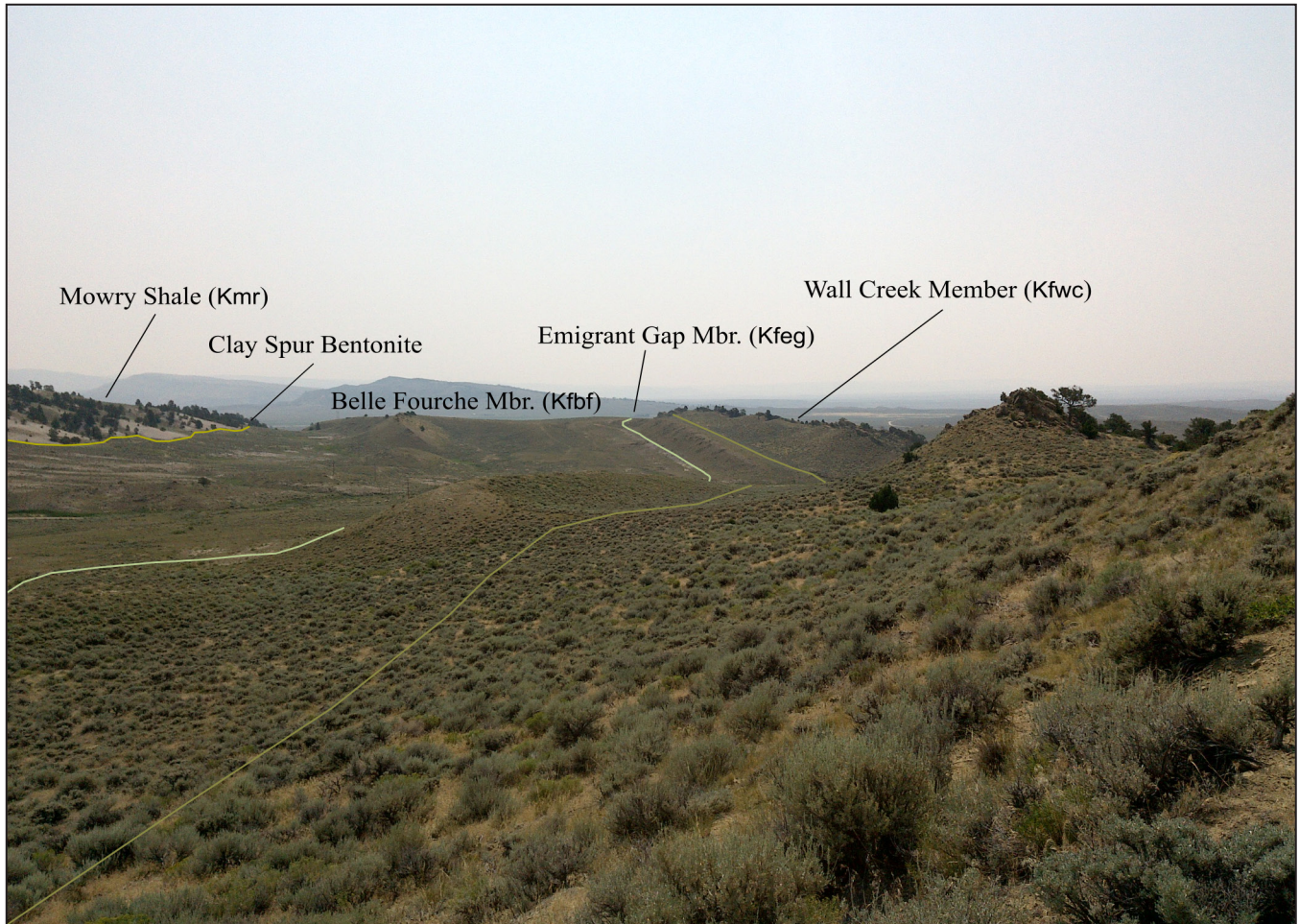


Figure 8. Annotated photograph of Mowry Shale and the Frontier Formation (Belle Fourche Member, Emigrant Gap Member, and Wall Creek Member). Looking southeast along strike, SE¼SE¼ sec. 34, T. 33 N., R. 82 W.



Figure 9. Photograph of Belle Fourche Member sandstone, looking east, SW $\frac{1}{4}$ SE $\frac{1}{4}$ sec. 7, T. 33 N. R. 82 W.



Figure 10. Photograph of chert-pebble conglomeratic sandstone in the Emigrant Gap Member of the Frontier Formation, NW $\frac{1}{4}$ SW $\frac{1}{4}$ sec. 36, T. 33 N., R. 82 W.



Figure 11. Photograph of the Wall Creek Member, looking northeast, NW $\frac{1}{4}$ SE $\frac{1}{4}$ sec. 22, T. 33 N., R. 82 W.

Sage Breaks Shale and Cody Shale

The Sage Breaks Shale often is not considered separately from the Cody Shale in the Wind River Basin (Lynds and Slattery, 2017); however, the “Sage Breaks equivalent” of Finn (2017), identified in nearby well logs, was readily identifiable in the field and therefore mapped as a separate unit (fig. 12). It is uncertain whether the contact of the Sage Breaks Shale with the overlying lower shaly member of the Cody Shale is conformable in the Oil Mountain quadrangle; the contact is sharp and is a known unconformity in the Powder River and Laramie basins (Lynds and Slattery, 2017).

The Cody Shale was a product of the Niobrara transgression-regression cycle, which inundated the continental interior in the late Turonian to early Coniacian, retreating in the early Campanian (Steidtmann, 1993). This was the longest lasting transgression of the Western Interior Seaway. The lower shaly member of the Cody Shale (fig. 13), a calcareous shale considered “Niobrara Formation equivalent” by Finn (2017), contains several chalky intervals that represent times of peak flooding (Steidtmann, 1993). The upper sandy member (fig. 14) is a thick noncalcareous shale interbedded with thin marine sandstones (Steidtmann, 1993). The lower shaly and upper sandy members of the Cody Shale are not mapped separately in the Oil Mountain quadrangle due to poor exposure.



Figure 12. Annotated photograph of streamcut of Sage Breaks Shale, looking northeast, SE¼SE¼ sec. 16, T. 33 N., R. 82 W.



Figure 13. Photograph of poorly exposed Cody Shale, looking southwest, NE $\frac{1}{4}$ SE $\frac{1}{4}$ sec. 33, T. 33 N., R. 82 W.



Figure 14. Photograph of upper Cody Shale sandstone, looking south, NW $\frac{1}{4}$ NW $\frac{1}{4}$ sec. 9, T. 32 N., R. 82 W.

Mesaverde Formation

The Mesaverde Formation was deposited during the Claggett transgression-regression cycle, during which a complex combination of tectonics, subsidence, sediment supply, and eustacy influenced sedimentation trends (Steidtmann, 1993).

In the early Campanian, as the Western Interior Seaway regressed eastward and sea levels stabilized, the basal member of the Mesaverde Formation, the Fales Sandstone, was deposited (Shapurji, 1978; Steidtmann, 1993). In the central Wind River Basin, the Fales Sandstone records littoral, nearshore marine, coastal swamp, fluvial, and lagoonal environments (Shapurji, 1978). Within the Oil Mountain quadrangle, the distal equivalents of these mostly terrestrial sediments were only exposed as thin, plane-bedded sandstones not readily distinguishable from the marine sandstones of the upper Cody Shale. For this reason, the existence, identity, and stratigraphic location of the Fales Sandstone in the Oil Mountain quadrangle was inferred from nearby well logs (Finn, 2007b).

As the sea advanced westward, sedimentation in the area briefly returned to offshore marine environments, resulting in deposition of the Wallace Creek Tongue of the Cody Shale (Shapurji, 1978). Then the sea again regressed eastward, and the Parkman Sandstone Member (fig. 15) was deposited in littoral and nearshore-marine environments (Shapurji, 1978; Steidtmann, 1993). Upsection, the unnamed middle member of the Mesaverde Formation

(figs. 16–17) was deposited in lagoonal, coastal swamp, and fluvial environments (Shapurji, 1978; Steidtmann, 1993). In the far eastern parts of the Wind River Basin, the unnamed middle member may contain a thin tongue of marine shale near its top, just below the base of the Teapot Sandstone (Finn, 2007b); these marine sediments were not observed in the Oil Mountain quadrangle due to either lack of exposure or absence of the facies as a whole. As the sea continued to regress eastward, the Teapot Sandstone (fig. 18) was deposited unconformably on a regional erosional surface in a series of coastal swamp, lagoonal, and fluvial environments (Gill and Cobban, 1966; Keefer, 1972; Steidtmann, 1993).



Figure 15. Photograph of Parkman Sandstone, looking southeast along strike, SW $\frac{1}{4}$ SE $\frac{1}{4}$ sec. 5, T. 32 N., R. 82 W.



Figure 16. Photograph of carbonaceous shales in the unnamed middle member of the Mesaverde Formation, looking south, NW $\frac{1}{4}$ NW $\frac{1}{4}$ sec. 5, T. 32 N., R. 82 W.



Figure 17. Photograph of the unnamed middle member of the Mesaverde Formation, looking northwest along strike, NW $\frac{1}{4}$ NE $\frac{1}{4}$ sec. 8, T. 32 N., R. 82 W.



Figure 18. Photograph of Teapot Sandstone of the Mesaverde Formation, looking southeast, NW $\frac{1}{4}$ NE $\frac{1}{4}$ sec. 8, T. 32 N., R. 82 W. The Teapot Sandstone forms a distinctive hogback ridge across the southwestern portion of the quadrangle.

Lewis Shale and Meeteetse Formation

The transgressions and regressions of the Bearpaw cycle deposited the marine Lewis Shale and intercalated terrestrial Meeteetse Formation (fig. 19; Steidtmann, 1993). The lower tongue of the Lewis Shale was deposited overlying the Teapot Sandstone in the late Campanian to early Maastrichtian during a major westward transgression of the seaway (Steidtmann, 1993). The Lewis Shale records deposition in shelf, slope, delta-front, turbidite, and basin-marine environments (Asquith, 1970; Steidtmann, 1993). Subsequent regression of the sea resulted in the deposition of the terrestrial sandstones, mudstones, siltstones, carbonaceous shales, and coals of the Meeteetse Formation (fig. 20) in low-lying fluvial, floodplain, paludal, lagoonal, deltaic, and coastal swamp environments (Keefer, 1965). With the next transgression of the sea, the upper tongue of the Lewis was deposited on the Meeteetse. The upper tongue of the Lewis Shale pinches out west of the Oil Mountain quadrangle (Keefer, 1965).

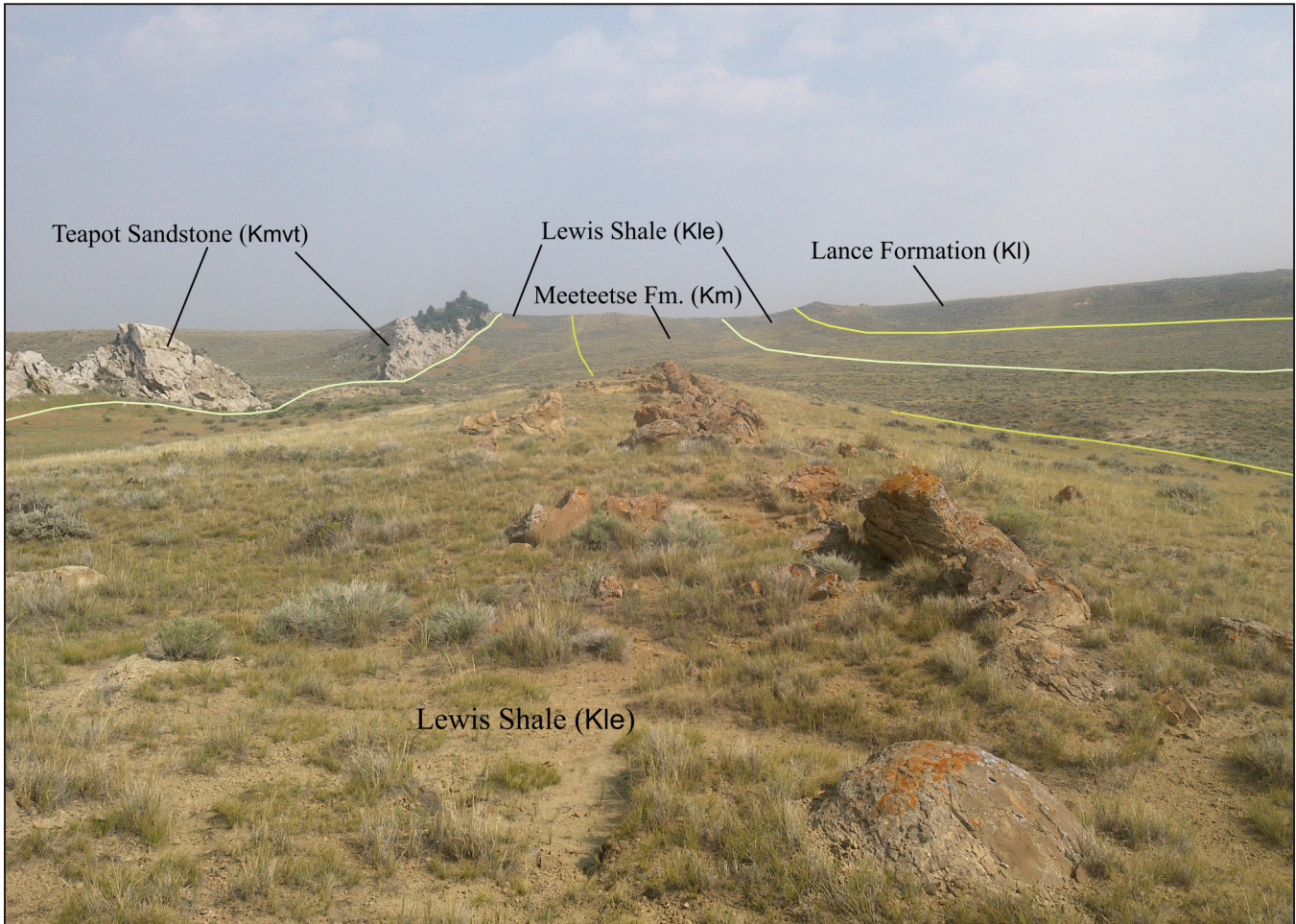


Figure 19. Annotated photograph of the Teapot Sandstone Member, Lewis Shale, Meeteetse Formation, and Lance Formation, looking southeast, SW $\frac{1}{4}$ NE $\frac{1}{4}$ sec. 31, T. 33 N., R. 82 W.

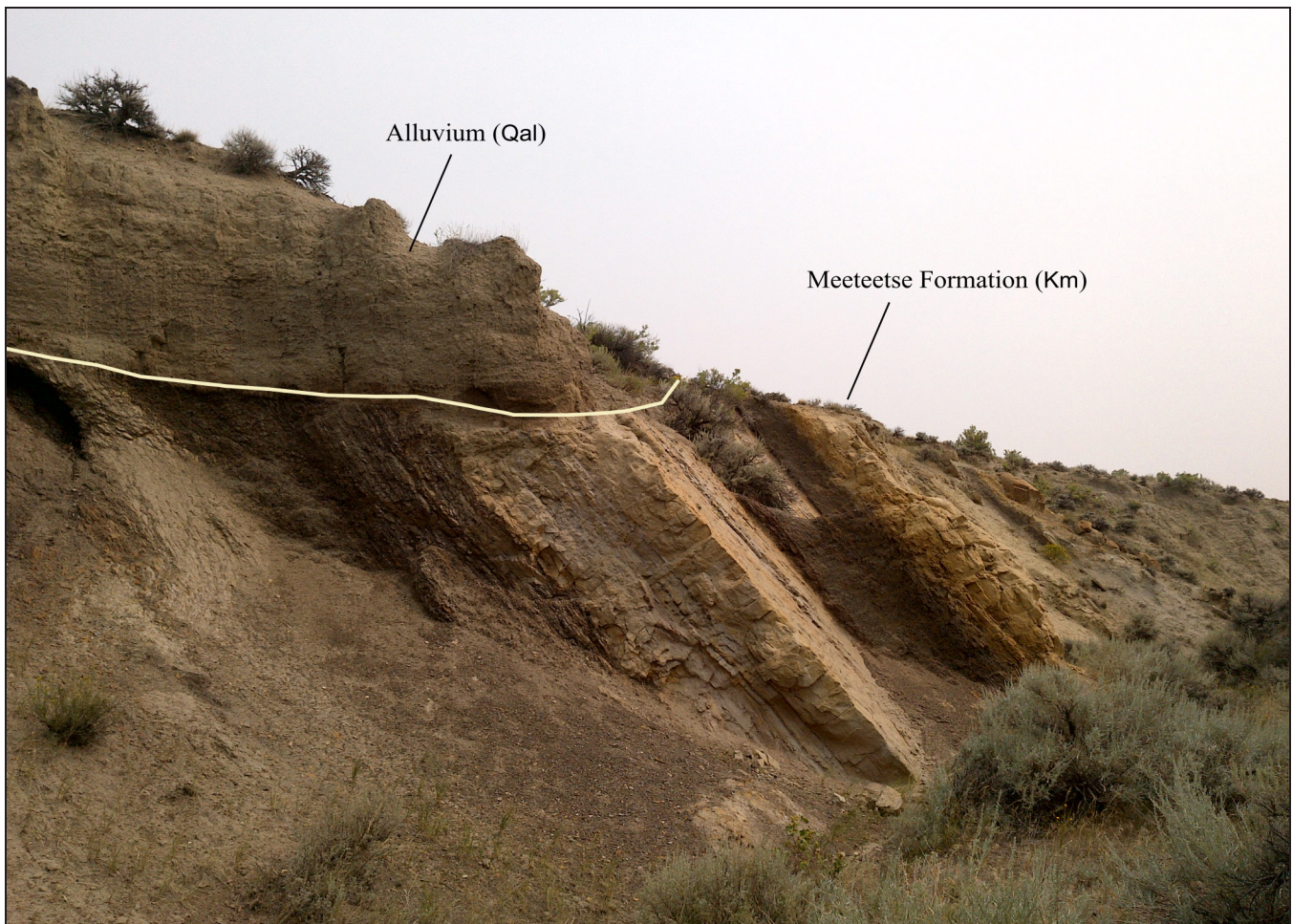


Figure 20. Annotated photograph of the Meeteetse Formation, looking south, NE $\frac{1}{4}$ NW $\frac{1}{4}$ sec. 8, T. 32 N., R. 82 W.

Lance Formation

During the onset of the Laramide orogeny, the Western Interior Seaway retreated for the final time, and the Sevier foreland basin was partitioned into Laramide basins by intervening Laramide uplifts. The Maastrichtian Lance Formation was deposited in a progression of coastal and terrestrial depositional environments in the rapidly subsiding trough of the Wind River Basin (Keefer and Love, 1963; Fan and Carrapa, 2014). Repeated delta facies in the lower Lance Formation (fig. 21) represent interdistributary bay deposits, whereas the upper Lance Formation (fig. 22) is dominated by channel sandstones and fine-grained paludal and lacustrine facies (Keefer, 1965; Gillespie and Fox, 1991; Johnson and others, 1996). Paleocurrent measurements show these river systems flowed northward across the Casper Arch, suggesting significant deformation of the Casper Arch did not occur until the Paleocene (Flemings and Nelson, 1991).



Figure 21. Photograph of interbedded sandstone, siltstone, coal, and carbonaceous shale in the lower Lance Formation, looking south, NW $\frac{1}{4}$ SE $\frac{1}{4}$ sec. 8, T. 32 N., R. 82 W.



Figure 22. Photograph of poorly exposed upper Lance Formation, looking east, SE $\frac{1}{4}$ SE $\frac{1}{4}$ sec. 36, T. 33 N., R. 83 W.

Fort Union Formation

The Paleocene Fort Union Formation lies unconformably on the Lance Formation (Keefer, 1965; Johnson, 2007). The sediments of the Fort Union Formation were laid down in fluvial, floodplain, paludal, marginal lacustrine, and lacustrine depositional environments (figs. 23–25; Keefer, 1965, 1969; Johnson, 2007). The variegated shales and mudstones record soil-forming processes. The deposition of channel sandstones near the formation's base occurred as river systems flowed northeast alongside the actively deforming Casper Arch (Flemings and Nelson, 1991; Johnson and others, 1996). Palynomorph biostratigraphy from this study and previous publications (Flemings and Nelson, 1991) suggest the very lowermost Fort Union Formation along the Casper Arch may actually be late Maastrichtian in age.

During the deposition of the fine-grained upper portion of the formation, considerable accommodation space was created by high rates of basin subsidence. Fort Union strata in the Oil Mountain quadrangle were deposited marginal to paleo-Waltman Lake, which occupied the northeastern part of the basin at this time (Keefer, 1965; Katz and Liro, 1993).



Figure 23. Photograph of lower Fort Union Formation, looking southeast along strike, SW $\frac{1}{4}$ SE $\frac{1}{4}$ sec. 6, T. 32 N., R. 82 W.



Figure 24. Photograph of the middle Fort Union Formation, looking east–northeast, downsection, NW¼NW¼ sec. 1, T. 32 N., R. 83 W.



Figure 25. Photograph of upper Fort Union Formation ferruginous pebble conglomerate outcrop, looking southeast along strike, NE¼NE¼ sec. 2, T. 32 N., R. 83 W.

Wind River Formation

Eocene deposition in the area began with deposition of a conglomeratic lower facies, bound both above and below by unconformities, and only occasionally present in descriptions of the area's geology. At the base of Clarkson Hill, about 8 km to the south, Rich (1962) maps a small exposure that he tentatively correlates with the Indian Meadows Formation of Love (1939) in the northwestern basin and the Lysite Member of Tourtelot (1948) in the north-central basin. He states that this "unit has a small areal distribution and has no lithologic equivalent in the adjoining areas," but it is unclear if he examined in detail the Oil Mountain quadrangle, where similar deposits were observed at the base of the escarpment in the southwestern corner of the map area.

For similar reasons of insufficient exposure, indeterminate age constraints, and uncertain correlation to either the Indian Meadows Formation or arkosic conglomerates in the upper Fort Union Formation (Rich, 1962), these coarse arkosic conglomerates and associated variegated floodplain deposits in the Oil Mountain quadrangle were mapped as part of the Wind River Formation. This lower facies was likely deposited during a pulse of Laramide activity, in alluvial fans, braided channels, and debris flows, as well as lakes, swamps, ponds, and floodplains (Seeland, 1978; Fan and others, 2011). Upsection, the deposits grade into a middle facies of predominantly floodplain deposits (fig. 26). Atop the escarpment to the southwest, the bulk of the area in the quadrangle mapped as Wind River Formation consists of the coarse-grained, poorly consolidated "upper coarse-grained facies" of Rich (1962). This unit consists of poorly exposed sandy soil with cobbles and small boulders of igneous and metamorphic rock (Seeland, 1978; Fan and others, 2011). Paleoclimate evidence in the Wind River Formation suggests a warm to hot savannah-type climate, which experienced annual wet and dry seasons (Seeland, 1978).



Figure 26. Photograph of Wind River Formation middle facies in foreground with lower Wind River Formation and Fort Union Formation in background, looking east, SW $\frac{1}{4}$ SE $\frac{1}{4}$ sec. 1, T. 32 N., R. 83 W.

Oligocene and Miocene formations

Younger rocks are known elsewhere in the region but are not preserved in the Oil Mountain quadrangle. The Oligocene White River Formation, where present, lies unconformably atop the Wind River Formation or older formations. It consists of conglomerate, conglomeratic sandstone, and tuffaceous siltstone and claystone. Its original thickness is unknown but is reported to be at least 843 ft (257 m) in the nearby Hiland-Clarkson Hill area (Rich, 1962).

In some locations in the region, Miocene-age strata unconformably overlie the White River Formation. These unnamed rocks, which correlate in part with the Split Rock Formation to the southwest, consist of interbedded conglomeratic sandstone and tuffaceous sandy siltstone and sandstone. Rich (1962) estimates a thickness of 1,000 to 1,500 ft (305 to 457 m) for these Miocene strata.

Regional uplift commenced in the late Miocene. Except for a few isolated Quaternary deposits, erosion and dissection has since defined the landscape around Oil Mountain.

Pleistocene terraces and aeolian deposits

Windblown sand was transported west to east across the Oil Mountain quadrangle during the Quaternary. Vegetated parabolic sand dunes overlie parts of the Frontier Formation and Cody Shale in the northern quadrangle. Dune-field activity spanning the last 20,000 years is documented throughout the Great Plains region; it is probable the isolated deposits in the Oil Mountain quadrangle share a history with the larger Casper Dune Field to the north and northeast, which was active in the early Holocene to as recently as about 4,000 years ago (Halfen and Johnson, 2013).

Pleistocene fluvial systems deposited terrace gravels throughout the Oil Mountain quadrangle (fig. 27). These flat benches represent relic river beds about 20 to 30 m above the modern grade of Poison Spider Creek. The clast composition of these elevated terraces is considerably more varied than the modern alluvium, and consists of various sedimentary, igneous, and metamorphic cobbles similar to those found in the upper facies of the Wind River Formation. Judging by their coarse grain size, the terraces were deposited by streams with considerably greater transport capacity than modern flows observed in the quadrangle.



Figure 27. Photograph of Pleistocene terrace, looking southeast, NE $\frac{1}{4}$ SW $\frac{1}{4}$ sec. 14, T. 33 N., R. 83 W.

Holocene alluvium and colluvium

Throughout the quadrangle, Holocene-age alluvium is still being actively deposited in streams and dry washes, and colluvium continues to accumulate at the base of slopes. These unconsolidated deposits are composed primarily of locally derived silt, sand, and pebbles.

ECONOMICS

Water Resources

Surface Water

There are three distinct drainages in the map area. As Natrona County receives an average of only 7 to 12 in (178 to 305 mm) of precipitation per year (Crist and Lowry, 1972), the only perennial natural stream in the quadrangle is Poison Spider Creek, which flows east across the north-central area of the map, south of Poison Spider field and about 2 km north of the Oil Mountain anticline. The Casper Canal is the other dominant water feature in the quadrangle. The canal begins about 25 km southwest of Oil Mountain at Alcova Reservoir, where in 1937 the U.S. Bureau of Reclamation completed the Alcova dam to supply irrigation water to the Casper-Alcova Irrigation District (Hein, 2014). In the Oil Mountain quadrangle, the Casper Canal bisects the Iron Creek anticline in the southeastern corner of the map and continues north through the Cody Shale.

Iron Creek and Clevidence Draw are two intermittent stream drainages in the map area. Iron Creek flows from west to east along the southern boundary of the quadrangle. No flow was observed in Iron Creek during the field season; however, the streambed accommodated green vegetation. The two branches of Clevidence Draw originate in the Wind River Formation and flow northeast toward the center of the map area, just north of the Oil Mountain anticline, where they join, cut through the Mowry Shale and Frontier Formation, and then flow east–northeast, joining Poison Spider Creek about 5 km east of the quadrangle.

Groundwater

Several geologic units exposed at the surface in the Oil Mountain quadrangle are known aquifers in the region: the Cloverly Formation, Muddy Sandstone, Mowry Shale, Frontier Formation, Cody Shale, Mesaverde Formation, Lewis Shale, Fort Union Formation, Wind River Formation, and Quaternary alluvium. Although lower Mesozoic and Paleozoic limestone formations, present only in the subsurface in the Oil Mountain quadrangle, may also act as aquifers, they are at considerable depth and therefore not addressed here. The following paragraphs discuss the potential yield and water quality of aquifers, based on an assessment of groundwater resources in Natrona County by Crist and Lowry (1972) of the U.S. Geological Survey. Publicly available water-quality analyses, from water wells and water-producing oil wells, are also summarized.

The Jurassic Morrison Formation in Natrona County is generally not an ideal aquifer due to its discontinuous sandstones and high concentrations of total dissolved solids (TDS; Crist and Lowry, 1972). In contrast, Crist and Lowry (1972) consider the Lower Cretaceous Cloverly Formation the most productive aquifer of the county's "Permian to Cretaceous aged continental and marine units," reporting a maximum of 250 gallons per minute (gpm) and an average of 5 to 20 gpm. However, the Cloverly Formation commonly has poor water quality, with high concentrations of TDS (Eschner and others, 1983). This formation typically cannot be used for domestic purposes and is largely unsuitable for irrigation unless it is freshly recharged near an outcrop and is used to water well-drained soils (Crist and Lowry, 1972).

Of the Upper Cretaceous section, the Frontier and Mesaverde formations are the most productive aquifers. Crist and Lowry (1972) report yields of up to 50 gpm for the Frontier Formation, but between one and 10 gpm is more typical (Crist and Lowry, 1972). Frontier Formation water can contain high sodium bicarbonate values, as much as 2,220 parts per million (ppm), likely due to carbonaceous material within the formation (Crist and Lowry, 1972).

The Mesaverde Formation has been used to supply water for livestock and is reported to yield up to 100 gpm but typically only 10 to 20 gpm (Crist and Lowry, 1972). In one instance, the Muddy Sandstone produced 45 gpm; like the Frontier Formation, the Muddy Sandstone may contain high sodium bicarbonate values, as great as 1,960 ppm, due to carbonaceous material (Crist and Lowry, 1972).

Other Cretaceous units in Natrona County do not have high potential for water-resource development. Although fracturing within the Mowry Shale is known to create secondary permeability, the formation typically has low yields, with a theoretical maximum of 20 gpm (Crist and Lowry, 1972). The Shannon and Sussex Sandstone members, which in the Oil Mountain quadrangle correlate with unnamed sandstones in the upper sandy member of the Cody Shale, can provide high yields, but the water may contain high levels of TDS and uranium (Rich, 1962; Crist and Lowry, 1972). The Lewis Shale, like other relatively low-permeability Cretaceous marine units, generally yields less than 10 gpm due to the discontinuous nature of its sandstones (Crist and Lowry, 1972).

Potential Paleogene-age aquifers in the Oil Mountain quadrangle include vast areal extents of terrestrial Paleocene and Eocene sedimentary deposits. Reported TDS in the Fort Union Formation in Natrona County range from 209 to 5,620 ppm, with a median concentration of 1,160 ppm (Eschner and others, 1983). The Wind River Formation typically produces around 25 gpm, although yields from 200 gpm to 350 gpm have been recorded (Whitcomb and Lowry, 1968; Crist and Lowry, 1972). Reported concentrations of TDS range from 276 to 1,830 ppm (Crist and Lowry, 1972). Bicarbonate in the Wind River Formation is increasingly prevalent at depth due to either carbonaceous material or sulfate reduction (Crist and Lowry, 1972). Water sourced from this formation can be used for irrigation but is typically limited to soils with good drainage (Crist and Lowry, 1972).

The Quaternary units in the Oil Mountain quadrangle include an assortment of windblown sand dunes, terrace gravels, and recent alluvium and colluvium. The water-resource characteristics of these deposits vary due to differences in source material, sorting, and location on the landscape. For instance, a terrace deposit consisting of resistant crystalline gravels is expected to have higher permeability than an alluvium deposit sourced from local shale and sandstone units. However, because many of the terrace deposits in the Oil Mountain quadrangle apron bedrock strath terraces along topographic highs, they may only act as impermanent or transient aquifers. Lastly, although Quaternary alluvium in Natrona County is known to be both high yielding and high quality (Crist and Lowry, 1972), many of the reported data are from along the North Platte River or tributaries not present in the Oil Mountain quadrangle.

In addition to often-elevated TDS concentrations, other contaminants may also be a concern, including nitrate, fluoride, and selenium. More than 85 percent of wells in Natrona County that have reported excess nitrate concentrations are in unconsolidated alluvium (Larson, 1984). Elevated fluoride is also known in Natrona County, and values exceeding 10 ppm are reported from the Fort Union and Frontier formations (Larson, 1984). Selenium, which is toxic to livestock above 0.5 ppm, has also been reported (Crist and Lowry, 1972; Larson, 1984). Weathering of Cretaceous shale bedrock, ubiquitous throughout the region and in the Oil Mountain quadrangle, is known to contribute to elevated selenium levels (Kulp and Pratt, 2004).

Wyoming State Engineer's Office records (Supplemental Data table 1) are available for six water-well permits in the Oil Mountain quadrangle, four of which were completed: two each for stock use and domestic groundwater (Wyoming State Engineer's Office, 2022). The reported flows ranged from 3 to 10 gpm, and the wells were drilled to depths ranging from 80 to 910 ft. Two of these wells were completed in the Wall Creek Member of the Frontier Formation, downdip of the eastern limb of the Poison Spider anticline. Aquifers of this configuration, where a water-bearing formation is present in the shallow subsurface downdip of nearby recharge areas, are sometimes conducive to improved yields and water quality. Of these two wells, the water quality for the well located 200 m downdip from outcrop of the Wall Creek Member was qualitatively noted as "good," whereas the well located about 2.2 km downdip from similar outcrop was considered "unsuitable for any use," with a TDS of 11,007 ppm. An artesian well is also noted on the U.S. Geological Survey topographic map in NE $\frac{1}{4}$ NE $\frac{1}{4}$ sec. 8, T. 33 N., R 82 W., about one km downdip from the same outcrop; no public data are known for this well.

Forty-four geochemical datasets for produced water from oil and gas wells are available in the quadrangle (Supplemental Data table 1; Blondes and others, 2019). Seventeen analyses are reported in Poison Spider field (six from the Tensleep Sandstone, seven from the Sundance Formation, four from the Cloverly Formation), 16 in Oil Mountain field (one from the Madison Limestone, 14 from the Tensleep Sandstone, one from the Cloverly Formation), seven in Iron Creek field (six from the Cloverly Formation, one from the Muddy Sandstone), one in Canal field (from the Frontier Formation), and five from wildcat wells (one from the Tensleep Sandstone, three from the Cloverly Formation, one from the Muddy Sandstone). TDS levels range from 1,311 ppm in the Cloverly Formation in Poison Spider field to 16,566 ppm in the Sundance Formation, also in Poison Spider field. Reported TDS levels in produced water in the quadrangle average 2,847 ppm. Additional produced-water data are available from the U.S. Geological Survey (Blondes and others, 2019).

Oil and Gas

Documented hydrocarbon production in the Oil Mountain quadrangle dates back to the mid-1800s, when axle grease for wagons and carts was produced from the oil seep at the northern end of the Oil Mountain anticline, in NE1/4 sec. 28, T. 33 N., R. 82 W. (Cserna and others, 1983; Fraser, 2015). Before this, indigenous peoples likely used oil from the seep for medicinal purposes and in paints (Fraser, 2015). The seep, from the Muddy Sandstone, is now dry. Several wildcat wells were drilled nearby in the 1950s with no success (Wyoming Oil and Gas Conservation Commission, 2022).

Iron Creek field, in the southeastern corner of the quadrangle, was discovered in 1917. As of February 2022, 379,000 barrels of oil and 3.7 million cubic feet of natural gas have been produced from the field (Wyoming Oil and Gas Conservation Commission, 2022). The primary reservoirs are the Muddy Sandstone, Frontier Formation, and Cloverly Formation, in an anticlinal closure along the crest of the Iron Creek anticline (Dahill, 1989a). The field currently contains 27 producing wells and 34 permanently abandoned wells. (The field extents on the map plate do not include wells that, although they may belong to a named-field designation in the Wyoming Oil and Gas Conservation Commission database, are outliers to the main field and might be better classified as wildcat wells.) The deepest well in this field reaches the Mississippian Madison Limestone.

Poison Spider field was also discovered in 1917. As of February 2022, 5.59 million barrels of oil and 65 million cubic feet of gas have been produced from the Sundance Formation, Muddy Sandstone, and Pennsylvanian Tensleep Sandstone (Wyoming Oil and Gas Conservation Commission, 2022). Production is from two independent closures along the symmetrically faulted, doubly plunging Poison Spider anticline (Dahill, 1989b). The field currently contains 58 producing wells, one active injection well, and 41 permanently abandoned wells. The deepest well in this field reaches Precambrian granite.

Oil Mountain field was discovered in 1945, and as of February 2022, 484,000 barrels of oil and 4.8 million cubic feet of gas have been produced from the Pennsylvanian Tensleep Sandstone (Motten, 1989; Wyoming Oil and Gas Conservation Commission, 2022). The field currently contains eight producing wells and eight permanently abandoned wells. The deepest well in this field reaches the Cambrian Flathead Sandstone.

Canal field was discovered in 1985. Production is from the Wall Creek Member of the Frontier Formation, although the initial target reservoir was the Muddy Sandstone. The trap is an updip pinch out of the sandstone reservoir (Specht, 1989), likely against west-vergent, east-dipping reverse faults antithetic to the northern segment of the west-dipping Iron Creek thrust. As of February 2022, 202,000 barrels of oil and 332 million cubic feet of gas have been produced from the field (Wyoming Oil and Gas Conservation Commission, 2022). The field currently contains two producing wells and 10 permanently abandoned wells.

Several wildcat wells have been drilled outside established fields in various parts of the quadrangle, with no or limited success.

Heavy-Mineral Sands

Heavy-mineral sands are mined worldwide for titanium, zirconium, and rare earth elements. They typically comprise Holocene placer deposits in unconsolidated coastal sands; however, some Cretaceous sandstones in Wyoming are also known to be enriched in heavy minerals. The geochemistry and mineralogy of these ancient shoreline deposits have been examined in various locations throughout Wyoming as potential sources for metal ores, rare earth elements, and other critical minerals (Dow and Batty, 1961; Houston and Murphy, 1962; Roehler, 1989; King, 1991; Sutherland and Cola, 2016; Lichtner and others, 2021).

Although the Oil Mountain quadrangle contains outcrop of Cretaceous stratigraphy known to contain heavy-mineral sandstones, no such deposits were observed. Ferruginous sandstones similar in appearance to heavy-mineral sandstones were seen in the Upper Cretaceous Mesaverde and Frontier formations as well as the Paleogene Fort Union and Wind River formations. Closer examination of select outcrops and samples did not show significant enrichment; however, a thorough survey of potential heavy-mineral sandstones in the quadrangle was not conducted.

Heavy-mineral sandstones are known to occur at the nearby Clarkson Hill, Poison Spider, and Ranger deposits. The Clarkson Hill deposit (sec. 20, T. 31 N., R. 82 W.) occurs roughly 12 km south of the Oil Mountain quadrangle, in the Parkman Sandstone of the Mesaverde Formation (Dow and Batty, 1961; Houston and Murphy, 1962). The Poison Spider deposit (sec. 1, T. 33 N., R. 84 W. and sec. 36, T. 34 N., R. 84 W.) is approximately 8–9 km west of the northeastern corner of the quadrangle (Dow and Batty, 1961; Sutherland and Cola, 2016); this deposit is reported to occur, somewhat unusually, in the Upper Cretaceous Lewis Shale, perhaps in a transitional coastal deposit near the contact of the lower tongue of the Lewis Shale with the intercalated, terrestrial Meeteetse Formation. The stratigraphic context of the Ranger deposit (sec. 22 and 27, T. 34 N., R. 84 W.), located about 12–13 km west of the northeastern corner of the quadrangle, is likewise unclear; this deposit is reported to occur in either the Lewis Shale or Lance Formation, perhaps in a transitional deposit near the contact between the two units (King, 1991).

Coal

Several formations in the Oil Mountain quadrangle are known to contain significant coal beds elsewhere in the Wind River Basin (Rieke and Kirr, 1984). Terrestrial and coastal deposits, such as in the Frontier, Mesaverde, Meeteetse, Lance, and Fort Union formations, have the potential to contain coal. Nearby mining for coal occurred at the Poison Spider mine in sec. 26, T. 33 N., R. 83 W., less than one km west of the Oil Mountain quadrangle (Horton and San Juan, 2022). This inactive mine produced small volumes of coal from the Meeteetse Formation and Lewis Shale.

Although carbonaceous shales were found throughout the Belle Fourche Member of the Frontier Formation, no significant coals were observed. Near its base the Teapot Sandstone Member of the Mesaverde Formation contains a laterally extensive thin coal. The Meeteetse Formation contains an approximately 1-m thick coal interbedded within floodplain and crevasse-splay deposits. The terrestrial deposits of the Lance Formation contain multiple thin coal horizons interbedded with lenticular sandstones, siltstone, carbonaceous shales, and mudstones. Coals observed in the Fort Union Formation were thin and in close proximity to carbonaceous shales and wood fragments.

Uranium

A scintillation monitor was used to assess outcrops for anomalous radioactivity during mapping of the quadrangle. No significant anomalies were detected; however, the Cloverly Formation in some locations did exhibit slightly elevated levels of radiation (about two times background). The inactive Dyper-Bar-Mac group uranium claims were located in a carbonaceous mudstone in the Cloverly Formation along the southwestern flank of the Oil Mountain anticline (King, 1991; Horton and San Juan, 2022). The Diamond M claim in the Wind River Formation is another inactive uranium claim in the quadrangle (Horton and San Juan, 2022).

Analysis of 15 whole rock samples from throughout the quadrangle returned overall low concentrations of uranium. The highest uranium values seen in the quadrangle were 7.62 ppm for a conglomerate in the Wind River Formation, 4.69 ppm in the basal conglomerate of the Cloverly Formation, and 3.46 ppm in the Sage Breaks Shale.

Industrial Minerals

While mineral extraction in the Oil Mountain quadrangle targets primarily oil, historically there has also been mining for aggregates and industrial minerals like bentonite clay. The regionally extensive Clay Spur Bentonite, a roughly 2-m-thick waxy yellow bentonitic clay at the top of the Mowry Shale, is a common target for industrial mineral extraction in the area. The Shell Creek Shale and Belle Fourche Member of the Frontier Formation also contain numerous bentonite beds.

The economic viability of bentonite deposits is partially determined by the angle of dip and the thickness of overlying rock. Bentonite beds that dip at low angles, typically around 10–15 degrees, and have low volumes of overburden are ideal targets for extraction (Dengo, 1946). In the Oil Mountain quadrangle, the Clay Spur Bentonite typically has dip values greater than 45 degrees. In some areas of the quadrangle the bed dips at about 30 degrees and has been mined in the past, such as at the Mills Bentonite Mine between Clevidence Draw and Poison Spider Creek (Sutherland and others, 2018).

Two aggregate operations are also documented in the Oil Mountain quadrangle. Mills pit and Poison Spider pit have sourced material from the Quaternary terrace gravels north of Poison Spider Road (Sutherland and others, 2018).

ANALYTICAL RESULTS

Geochemistry

Fifteen samples were analyzed for major- and trace-element geochemistry. A few of the more interesting results are briefly mentioned here. It should be noted that the word “elevated” refers only to a concentration above that of typical upper continental crust and does not imply an economic deposit. Geochemical data and related sample information are provided in Supplemental Data table 2.

A pebble conglomerate in the lower Wind River Formation (OM-DL-20210804-1A) exhibited slightly elevated levels of thorium, uranium, rare earth elements, cobalt, and nickel. A carbonate concretion in the Sage Breaks Shale (OM-DL-20210803-4A) contained slightly elevated lithium, vanadium, and chromium. A number of samples—from the Morrison Formation (OM-DL-20210727-1ABC), Belle Fourche Member (OM-DL-20210819-1A), Emigrant Gap Member (OM-DL-20210729-5A, OM-DL-20210729-6A), Wall Creek Member (OM-DL-20210727-7A), Cody Shale (OM-DL-20210803-4A, OM-DL-20210803-4B), Teapot Sandstone (OM-DL-20210728-6A), Lance Formation (OM-DL-20210806-1A), Fort Union Formation (OM-DL-20210804-4A, OM-DL-20210804-6A), and Wind River Formation (OM-DL-20210804-1A)—exhibited elevated selenium concentrations.

Source-Rock Analysis

Total organic carbon (TOC) and programmed pyrolysis measurements were collected for seven samples from formations that are known or potential oil and gas source rocks in the Wind River and Powder River basins. TOC values ranged from 0.73 in the upper Cody Shale to 3.18 in the Mowry Shale. A majority of the samples contained Type IV inert kerogen. The two most organic-rich samples (OM-DL-20210803-3A, lower Cody Shale; OM-DL-20210805-4A, Mowry Shale) contain mixed Type II-III kerogen. Overall, the source-rock analysis results are comparable to data from Finn (2007a) in the southeastern Wind River Basin.

Total organic carbon and programmed pyrolysis results are summarized in table 1.

Table 1. Source-rock analysis results. Latitude and longitude are displayed in GCS NAD27.

Sample name	Map station	Geologic unit	Latitude	Longitude	TOC (wt. %)	S1 (mg/g)	S2 (mg/g)	S3 (mg/g)	Hydrogen index (HI)	Oxygen index (OI)	Tmax (°C)
OM-DL-20210728-2A	OM04	Kc (upper)	42.77989	-106.67550	0.73	0.41	0.28	0.49	38	67	332
OM-DL-20210803-3A	OM14	Kc (lower)	42.82508	-106.64782	2.32	0.09	5.35	1.37	230	59	423
OM-DL-20210803-4B	OM15	Ksb	42.82371	-106.67417	0.83	0.02	0.26	0.7	31	84	437
OM-JK-20210805-1A	OM40	Kfbf	42.80535	-106.68736	1.53	0.02	0.67	0.6	44	39	426
OM-DL-20210805-2A	OM29	Kmr	42.80612	-106.68532	1.24	0.02	0.54	0.92	44	74	428
OM-DL-20210805-4A	OM30	Kmr	42.80537	-106.68587	3.18	0.25	6.73	1.86	212	58	420
OM-DL-20210805-5A	OM31	Kmr	42.80534	-106.68937	1.43	0.01	0.85	1.06	59	74	430

Palynomorph Biostratigraphy

Palynological analysis of 12 samples from the Meeteetse Formation through the Wind River Formation was conducted by Biostratigraphy.com, LLC to constrain the age of deposition of uppermost Cretaceous and Paleogene syn-Laramide terrestrial sediments, and to provide insight as to environment at the time of deposition. Interpretations of depositional age ranged from Late Campanian to Early Eocene.

The results are summarized in table 2. Detailed palynomorph counts are provided in Supplemental Data tables 3–14.

Table 2. Depositional ages determined from palynomorph biostratigraphy.

Sample name	Map station	Geologic unit	Latitude	Longitude	Age limits from palynomorph biostratigraphy		Confidence
					lower	upper	
OM-DL-20210831-3A	OM39	Twdr	42.76452	-106.72666	Paleocene	Late Oligocene	low
OM-DL-20210804-2A	OM21	Twdr	42.77487	-106.73947	Paleocene	Early Oligocene	moderate
OM-DL-20210804-3A	OM22	Tfu	42.77512	-106.73924	Late Paleocene	Early Eocene	high
OM-DL-20210804-5A	OM24	Tfu	42.77655	-106.73679	Maastrichtian	Late Paleocene	moderate
OM-DL-20210804-7A	OM26	Tfu	42.77723	-106.73612	Early Paleocene	Early Paleocene	moderate–high
OM-DL-20210804-8A	OM27	Tfu	42.77739	-106.73212	Earliest Paleocene	Late Maastrichtian	high
OM-DL-20210804-9A	OM28	Tfu	42.77783	-106.73068	Latest Maastrichtian	Latest Maastrichtian	high
OM-DL-20210806-1A	OM32	Kl	42.76388	-106.70128	Maastrichtian	Late Maastrichtian	high
OM-DL-20210831-2A	OM38	Kl	42.76495	-106.69770	Late Maastrichtian	Late Maastrichtian	high
OM-DL-20210831-1A	OM37	Kl	42.76457	-106.69555	Late Campanian	Late Maastrichtian	moderate
OM-DL-20210830-3A	OM36	Kl	42.75887	-106.69035	Late Campanian	Late Maastrichtian	moderate
OM-DL-20210830-2A	OM35	Km	42.76203	-106.68911	Maastrichtian	Late Maastrichtian	moderate

Detrital Zircon Geochronology

To constrain depositional age, as well as to contribute to public datasets for use in interpreting provenance and Laramide tectonics, detrital zircons in rock samples from the Lance, Fort Union, and Wind River formations were dated with U-Pb geochronology at the Arizona LaserChron Center at the University of Arizona. Data were processed with IsoplotR (Versmeech, 2018). Sample locations and youngest-single-grain ages are summarized in table 3. Detrital zircon age distributions are shown in fig. 28. The complete dataset is available in Supplemental Data tables 15–17.

Preliminary, qualitative comments on the results are given here. The ages of detrital zircons in the samples range from Late Cretaceous to Archean. Cretaceous-age zircons dominate, reflecting Sevier magmatic arc and batholith sources. Paleoproterozoic Yavapai-Mazatzal terrane zircons are also numerous. The zircon age distributions of both the Lance and Fort Union formation samples likely reflect recycling of a wide age range of zircons from sedimentary rocks in the Sevier orogenic belt and incipient Laramide uplifts; in contrast, the Wind River Formation sample

shows a markedly increased number of Archean-age zircons, likely from primary Wyoming Craton sources exposed during uplift and unroofing of the Granite Mountains and other nearby Laramide uplifts in the early Eocene (Fan and others, 2011).

Although the youngest grains in each sample reflect the expected relative ages of the formations, these maximum depositional ages do not converge to the actual depositional ages suggested by regional correlations (Lynds and Slattery, 2017). All calculated maximum depositional ages appear to be a few million years older than the actual time of deposition.

Table 3. Detrital zircon sample locations and youngest-single-grain ages. Uncertainties shown in these results are at the 1σ level and include only measurement error. The complete digital dataset is available in the Supplemental Data.

Sample name	Map station	Geologic unit	Latitude	Longitude	Youngest single grain (Ma)	+/- (Ma, 1σ)
OM-DL-20210804-1A	OM20	Twdr	42.77459	-106.73945	68.8	0.6
OM-DL-20210804-6A	OM25	Tfu	42.77718	-106.73612	71.1	0.7
OM-DL-20210806-1A	OM32	Kl	42.76388	-106.70128	73.1	0.9

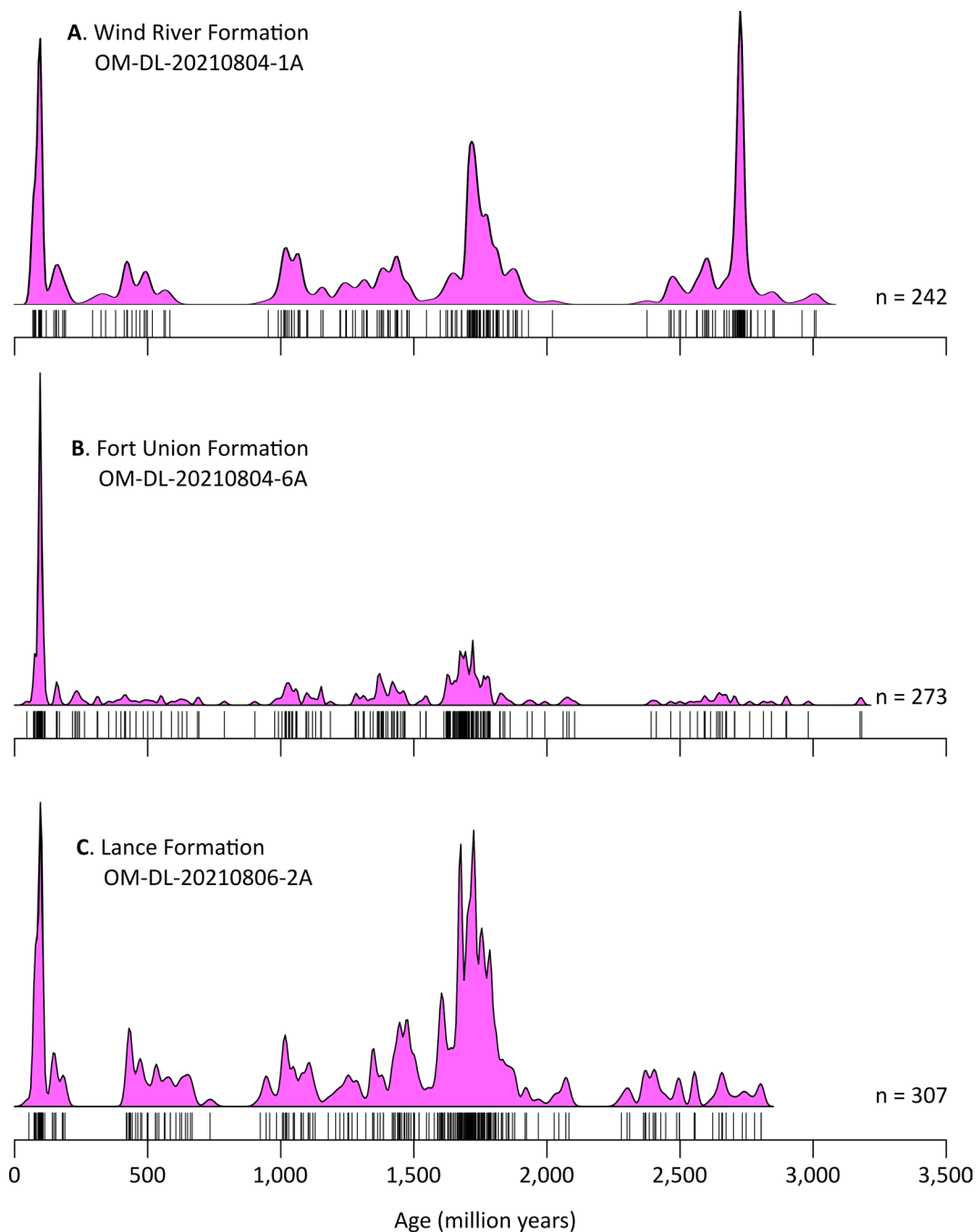


Figure 28. Kernel density estimate (KDE) plots of detrital zircon age distributions for (A) Wind River Formation, (B) Fort Union Formation, and (C) Lance Formation samples.

ACKNOWLEDGMENTS

Geologic mapping of the Oil Mountain quadrangle would not have been possible without the generous permission of the private landowners who granted access to scientists from the Wyoming State Geological Survey. In particular, we owe thanks to Mills Livestock Company, Len Camp, Pacificorp, and YZ Limited Partnership.

Preparation of this map and report was supported the U.S. Geological Survey, National Cooperative Geologic Mapping Program, under USGS award number G21AC10538.

REFERENCES

- Asquith, D.O., 1970, Depositional topography and major marine environments, Late Cretaceous, Wyoming: American Association of Petroleum Geologists Bulletin, v. 54, no. 7, p. 1,184–1,224.
- Blondes, M.S., Gans, K.D., Engle, M.A., Kharaka, Y.K., Reidy, M.E., Saraswathula, Varun, Thordsen, J.J., Rowan, E.L., and Morrissey, E.A., 2019, U.S. Geological Survey National Produced Waters Geochemical Database v2.3: U.S. Geological Survey Data Release.
- Carroll, A.R., Chetel, L.M., and Smith, M.E., 2006, Feast to famine—Sediment supply control on Laramide basin fill: *Geology*, v. 34, no. 3, p. 197–200.
- Crist, M.A., and Lowry, M.E., 1972, Ground-water resources of Natrona County, Wyoming: U.S. Geological Survey Water Supply Paper 1897, 92 p., 3 pls.
- Cserna, E.G., Kerns, G.J., and Laraway, W.J., 1983, Bedrock geologic map of the Pine Mountain-Oil Mountain area, Natrona County, Wyoming: U.S. Geological Survey Open-File Report 83-748, 18 p., 4 pls., scale 1:31,680.
- Curry, W.H., III, 1985, Grieve paleovalley of the Muddy Sandstone in the eastern Wind River Basin, Wyoming, *in* Nelson, G.E., ed., *The Cretaceous geology of Wyoming: Wyoming Geological Association, 36th annual field conference, Guidebook*, p. 75–79.
- Dahill, M.P., 1989a, Iron Creek, *in* Cardinal, D.F., Miller, Terry, Stewart, W.W., and Trotter, J.F., eds., *Bighorn and Wind River basins: Wyoming Geological Association, Oil and gas field symposium*, p. 244–246.
- _____, 1989b, Poison Spider, *in* Cardinal, D.F., Miller, Terry, Stewart, W.W., and Trotter, J.F., eds., *Bighorn and Wind River basins: Wyoming Geological Association, Oil and gas field symposium*, p. 376–378.
- DeCelles, P.G., 2004, Late Jurassic to Eocene evolution of the Cordilleran thrust belt and foreland Basin system, western U.S.A: *American Journal of Science*, v. 304, p. 105–168.
- Dengo, Gabriel, 1946, Geology of bentonite deposits near Casper, Natrona County, Wyoming: Geological Survey of Wyoming [Wyoming State Geological Survey] Bulletin 37, 25 p., 3 pls.
- Dow, V.T., and Batty, J.V., 1961, Reconnaissance of titaniferous sandstone deposits in Utah, Wyoming, New Mexico, and Colorado: U.S. Bureau of Mines Report of Investigations 5860, 52 p.
- English, J.M., and Johnston, S.T., 2004, The Laramide orogeny—What were the driving forces?: *International Geology Review*, v. 46, no. 9, p. 833–838.
- Eschner, T.R., Hadley, R.F., and Crowley, K.D., 1983, Hydrologic and morphologic changes in the channels of the Platte River basin in Colorado, Wyoming and Nebraska—A historical perspective: U.S. Geological Survey Professional Paper 1277-A, 39 p.
- Fraser, Allan, 2015, Oil seeps and axle grease—Petroleum sales on the emigrant trails: Wyoming State Historical Society, accessed April 2022, at <https://www.wyohistory.org/encyclopedia/oil-seeps-and-axle-grease-petroleum-sales-emigrant-trails>.
- Fan, Majie, and Carrapa, Barbara, 2014, Late Cretaceous–early Eocene Laramide uplift, exhumation, and basin subsidence in Wyoming—Crustal responses to flat slab subduction: *Tectonics*, v. 33, no. 4, p. 509–529.
- Fan, Majie, DeCelles, P.G., Gehrels, G.E., Dettman, D.L., Quade, Jay, and Peyton, S.L., 2011, Sedimentology, detrital zircon geochronology, and stable isotope geochemistry of the lower Eocene strata in the Wind River Basin, central Wyoming: *Geological Society of America Bulletin*, v. 123, no. 5–6, p. 979–996.
- Flemmings, P.B., and Nelson, S.N., 1991, Paleogeographic evolution of the latest Cretaceous and Paleocene Wind River Basin: *The Mountain Geologist*, v. 28, p. 36–52.

- Finn, T.M., 2007a, Source rock potential of upper cretaceous marine shales in the Wind River Basin, Wyoming, chap. 8 of U.S. Geological Survey Wind River Basin Province Assessment Team, comp., Petroleum systems and geologic assessment of oil and gas in the Wind River Basin province, Wyoming: U.S. Geological Survey Digital Data Series DDS-69-J, 24 p.
- _____, 2007b, Subsurface stratigraphic cross sections of Cretaceous and Lower Tertiary rocks in the Wind River Basin, central Wyoming, chap. 9 of U.S. Geological Survey Wind River Basin Province Assessment Team, comp., Petroleum systems and geologic assessment of oil and gas in the Wind River Basin province, Wyoming: U.S. Geological Survey Digital Data Series DDS-69-J, 28 p., 11 pls.
- _____, 2017, Stratigraphic cross sections of the Niobrara interval of the Cody Shale and associated rocks in the Wind River Basin, central Wyoming: U.S. Geological Survey Scientific Investigations Map 3370, 19 p., 1 pl.
- General Petroleum Corporation, 1954, Geological map of South Casper Creek, Poison Spider, Oil Mountain, Iron Creek, Natrona County, Wyoming, scale 1:36,026, *in* Olson, W.G., ed.: Wyoming Geological Association, ninth annual field conference, Guidebook, 83 p., 10 pls.
- Gill, J.R., and Cobban, W.A., 1966, Regional unconformity in Late Cretaceous, Wyoming: U.S. Geological Survey Professional Paper 550-B, p. B20–B27.
- Gillespie, J.M., and Fox, J.E., 1991, Tectonically influenced sedimentation in the Lance Formation, eastern Wind River Basin, Wyoming: *The Mountain Geologist*, v. 28, no. 2-3, p. 53–66.
- Halfen, A.F., and Johnson, W.C., 2013, A review of Great Plains dune field chronologies: *Aeolian Research*, v. 10, p. 135–160.
- Hares, C.J., Ball, M.W., Clair, S.S., Reeside, J.B., Heald, K.C., and Collins, A.C., 1946, Geologic map of the southeastern part of the Wind River Basin and adjacent areas in central Wyoming: U.S. Geological Survey Preliminary Map 51, scale 1:126,720.
- Harshman, E.N., 1972, Geology and uranium deposits, Shirley Basin area, Wyoming: U.S. Geological Survey Professional Paper 745, 82 p.
- Hennings, P.H., Olson, J.E., and Thompson, L.B., 2000, Combining outcrop data and three-dimensional structural models to characterize fractured reservoirs—An example from Wyoming: *American Association of Petroleum Geologists Bulletin*, v. 84, no. 6, p. 830–849.
- Hein, Annette, 2014, Alcova dam and reservoir: Wyoming State Historical Society, accessed April 2022, at <https://www.wyohistory.org/encyclopedia/alcova-dam-and-reservoir>.
- Hintze, F.F., 1915, The Basin and Greybull oil and gas fields: Wyoming Geological Survey [Wyoming State Geological Survey] Bulletin 10, 62 p.
- Horton, J.D., and San Juan, C.A., 2022, Prospect- and mine-related features from U.S. Geological Survey 7.5- and 15-minute topographic quadrangle maps of the United States (ver. 7.0, April 2022): U.S. Geological Survey Data Release.
- Houston, R.S., and Murphy, J.R., 1962, Titaniferous black sandstone deposits of Wyoming: Geological Survey of Wyoming [Wyoming State Geological Survey] Bulletin 49, 120 p., 15 pls.
- Hunter, John, Ver Ploeg, A.J., and Boyd, C.S., 2005, Geologic map of the Casper 30' x 60' quadrangle, Natrona and Converse counties, central Wyoming: Wyoming State Geological Survey Map Series 65, scale 1:100,000.
- Johnson, R.C., 2007, Detailed measured sections, cross sections, and paleogeographic reconstructions of the Upper Cretaceous and Lower Tertiary non-marine interval, Wind River Basin, Wyoming, chap. 10 of U.S. Geological Survey Wind River Basin Province Assessment Team, comp., Petroleum systems and geologic assessment of oil and gas in the Wind River Basin province, Wyoming: U.S. Geological Survey Digital Data Series DDS-69-J, 43 p., 6 pls.

- Johnson, R.C., Finn, T.M., Keefer, W.R., and Szmajter, R.J., 1996, Geology of Upper Cretaceous and Paleocene gas-bearing rocks, Wind River Basin, Wyoming: U.S. Geological Survey Open-File Report 96-90, 120 p., 3 pls.
- Katz, B.J., and Liro, L.M., 1993, The Waltman Shale Member, Fort Union Formation, Wind River Basin—A Paleocene clastic lacustrine source system, *in* Keefer, W.R., Metzger, W.J., and Godwin, L.H., eds., Oil and gas and other resources of the Wind River Basin, Wyoming: Wyoming Geological Association Special Symposium, p. 163–174.
- Keefer, W.R., 1965, Stratigraphy and geologic history of the uppermost Cretaceous, Paleocene, and Lower Eocene rocks in the Wind River Basin, Wyoming: U.S. Geological Survey Professional Paper 495-A, p. 77 p., 4 pls., scale 1:289,700.
- _____, 1969, General stratigraphy and depositional history of the Fort Union, Indian Meadows, and Wind River formations, Wind River Basin, Wyoming, *in* Barlow, J.A., ed., Symposium on Tertiary rocks of Wyoming: Wyoming Geological Association, 21st annual field conference, Guidebook, p. 19–28.
- _____, 1970, Structural geology of the Wind River Basin, Wyoming: U.S. Geological Survey Professional Paper 495-D, 35 p., 3 pls., scale 1:250,000.
- _____, 1972, Frontier, Cody, and Mesaverde formations in the Wind River and southern Bighorn basins, Wyoming: U.S. Geological Survey Professional Paper 495-E, 22 p., 3 pls.
- Keefer, W.R., and Love, J.D., 1963, Laramide vertical movements in central Wyoming: *Rocky Mountain Geology*, v. 2, no. 1, p. 47–54.
- King, J.K., 1991, Rare earth elements and yttrium in Wyoming: Wyoming State Geological Survey Industrial Minerals Report 91-3, 125 p. (Supersedes Geological Survey of Wyoming Open File Report 87-8; Revised by R.E. Harris 2002).
- Kulp, T.R., and Pratt, L.M., 2004, Speciation and weathering of selenium in upper cretaceous chalk and shale from South Dakota and Wyoming, USA: *Geochimica et Cosmochimica Acta*, v. 68, no. 18, p. 3,687–3,701.
- Larson, L.R., Ground-water quality in Wyoming: U.S. Geological Survey Water-Resources Investigations Report 4034, 71 p.
- Li, Zhiyang, and Aschoff, Jennifer, 2022, Shoreline evolution in the Late Cretaceous North American Cordilleran foreland basin—An exemplar of the combined influence of tectonics, sea level, and sediment supply through time: *Earth-Science Reviews*, v. 226, 32 p.
- Lichtner, D.T., Gay, G.W., and Kehoe, K.S., 2021, Heavy-mineral sandstone in the Upper Cretaceous Rock Springs Formation, Richards Gap, Wyoming: Wyoming State Geological Survey Open File Report 2021-6, 37 p.
- Liu, Lijun, Gurnis, Michael, Seton, Maria, Saleeby, Jason, Müller, R.D., and Jackson, J.M., 2010, The role of oceanic plateau subduction in the Laramide orogeny: *Nature Geoscience*, v. 3, p. 353–357.
- Love, J.D., 1939, Geology along the southern margin of the Absaroka Range, Wyoming: Geological Society of America Special Paper 20, 134 p., 17 pls.
- _____, 1948, Mesozoic stratigraphy of the Wind River Basin, central Wyoming, *in* Maebius, J.B., and Netterstrom, P.W., eds., Wind River Basin, Wyoming: Wyoming Geological Association, third annual field conference, Guidebook, p. 96–111.
- Lupton, C.T., 1916, Oil and gas near Basin, Big Horn County, Wyoming: U.S. Geological Survey Bulletin, v. 621, p. 157–190.
- Lynds, R.M., and Slattery, J.S., 2017, Correlation of the Upper Cretaceous strata of Wyoming: Wyoming State Geological Survey Open File Report 2017-3.
- McMillan, M.E., Heller, P.L., and Wing, S.L., 2006, History and causes of post-Laramide relief in the Rocky Mountain orogenic plateau: *Geological Society of America Bulletin*, v. 118, no. 3-4, p. 393–405.

- Merewether, E.A., 1983, The Frontier Formation and mid-Cretaceous orogeny in the foreland of southwestern Wyoming: *The Mountain Geologist*, v. 20, no. 4, p. 121–138.
- Merewether, E.A., and Cobban, W.A., 1986, Evidence of mid-Cretaceous tectonism in the Frontier Formation, Natrona County, Wyoming: *Earth Science Bulletin*, v. 19, p. 142–152.
- Merewether, E.A., Cobban, W.A., and Cavanaugh, E.T., 1979, Frontier Formation and equivalent rocks in eastern Wyoming: *The Mountain Geologist*, v. 16, no. 3, p. 67–102.
- Minor, K.P., Steel, R.J., and Olariu, Cornel, 2022, Tectonic and eustatic control of Mesaverde Group (Campanian–Maastrichtian) architecture, Wyoming-Utah-Colorado region, USA: *Geological Society of America Bulletin*, v. 134, no. 1-2, p. 419–445.
- Motten, Roger, 1989, Oil Mountain, *in* Cardinal, D.F., Miller, Terry, Stewart, W.W., and Trotter, J.F., eds., Bighorn and Wind River basins: Wyoming Geological Association, Oil and gas field symposium, p. 338–339.
- Nichols, D.J., 2003, Palynostratigraphic framework for age determination and correlation of the nonmarine lower Cenozoic of the Rocky Mountains and Great Plains region, *in* Reynolds, R.G., and Flores, R.M., eds., *Cenozoic systems of the Rocky Mountain region: Rocky Mountain Section Society for Sedimentary Geology Rocky Mountain Section Special Publication*, p. 107–134.
- Nightengale, E.J., 1990, Structural and stress analysis of the Oil Mountain anticline, Natrona County, Wyoming: Akron, Ohio, University of Akron, M.S. thesis, 69 p.
- Picard, M.D., 1993, The early Mesozoic history of Wyoming, *in* Snoke, A.W., Steidtmann, J.R., and Roberts, S.M., eds., *Geology of Wyoming: Geological Survey of Wyoming [Wyoming State Geological Survey] Memoir 5*, p. 210–248.
- Rich, E.I., 1962, Reconnaissance geology of Hiland-Clarkson Hill area, Natrona County, Wyoming: *U.S. Geological Survey Bulletin 1107-G*, p. 447–537, 4 pls., scale 1:31,680.
- Rieke, H.H., and Kirr, J.N., 1984, Geologic overview, coal, and coalbed methane resources of the Wind River Basin—Wyoming, *in* Coalbed methane resources of the United States: American Association of Petroleum Geologists *Studies in Geology* 17, p. 295–334.
- Roehler, H.W., 1989, Origin and distribution of six heavy-mineral placer deposits in coastal-marine sandstones in the Upper Cretaceous McCourt Sandstone Tongue of the Rock Springs Formation, southwest Wyoming: *U.S. Geological Survey Bulletin 1867*, 34 p., 1 pl.
- Seeland, David, 1978, Sedimentology and stratigraphy of the lower Eocene Wind River Formation, central Wyoming, *in* Boy, R.G., Olson, G.M., and Boberg, W.W., eds., *Resources of the Wind River Basin: Wyoming Geological Association, 30th annual field conference, Guidebook*, p. 181–198.
- Shapurji, S.S., 1978, Depositional environments and correlation of the Mesaverde Formation, Wind River Basin, Wyoming, *in* Boyd, R.G., Olson, G.M., and Boberg, W.W., eds., *Resources of the Wind River Basin: Wyoming Geological Association, 30th annual field conference, Guidebook*, p. 167–180.
- Specht, R.G., 1989, Canal, *in* Cardinal, D.F., Miller, Terry, Stewart, W.W., and Trotter, J.F., eds., Bighorn and Wind River basins: Wyoming Geological Association, Oil and gas field symposium, p. 86–87.
- Steidtmann, J.R., 1993, The Cretaceous foreland basin and its sedimentary record, *in* Snoke, A.W., Steidtmann, J.R., and Roberts, S.M., eds., *Geology of Wyoming: Geological Survey of Wyoming [Wyoming State Geological Survey] Memoir 5*, p. 250–271.
- Stone, D.S., 2002, Morphology of the Casper Mountain uplift and related subsidiary structures, central Wyoming—Implications for Laramide kinematics, dynamics, and crustal inheritance: *American Association of Petroleum Geologists Bulletin*, v. 86, no. 8, p. 1,417–1,440.
- Sutherland, W.M., and Cola, E.C., 2016, A comprehensive report on rare earth elements in Wyoming: Wyoming State Geological Survey Report of Investigations 71, 137 p.

- Sutherland, W.M., Stafford, J.E., Carroll, C.J., Gregory, R.W., and Kehoe, K.S., 2018, Mines and minerals map of Wyoming: Wyoming State Geological Survey, accessed April 2022, at <https://wsgs.maps.arcgis.com/apps/webappviewer/index.html?id=af948a51f4954a81adeae8935440cd28>.
- Thompson, R.C., 2015, Post-Laramide, collapse-related fracturing and production, Wind River Basin, Wyoming: *The Mountain Geologist*, v. 52, no. 4, p. 27–46.
- Tourtlot, H.A., 1948, Tertiary rocks in the northeastern part of the Wind River Basin, Wyoming, *in* Maebius, J.B., and Netterstrom, P.W., Wind River Basin, Wyoming: Wyoming Geological Association, third annual field conference, Guidebook, p. 112–124.
- Versmeech, Pieter, 2018, IsoplotR—A free and open toolbox for geochronology: *Geoscience Frontiers*, v. 9, no. 5, p. 1,479–1,493.
- Whitcomb, H.A., and Lowry, M.E., 1968, Ground-water resources and geology of the Wind River Basin area, central Wyoming: U.S. Geological Survey Hydrologic Atlas 270, 14 p., 3 pls.
- Wyoming Oil and Gas Conservation Commission, 2022, Wyoming Oil and Gas Conservation Commission, accessed March 2022, at <https://wogcc.wyo.gov/data>.
- Wyoming State Engineer's Office, 2022, Wyoming State Engineer's Office, accessed March 2022, at <http://seoweb.wyo.gov/e-Permit/Common/Login.aspx>.

